

[advances.sciencemag.org/cgi/content/full/6/14/eaaz7825/DC1](https://advances.sciencemag.org/cgi/content/full/6/14/eaaz7825/DC1)

## Supplementary Materials for

### **Epitope-directed antibody selection by site-specific photocrosslinking**

Longxin Chen, Chaoyang Zhu, Hui Guo, Runting Li, Limeng Zhang, Zhenzhen Xing, Yue Song, Zihan Zhang, Fuping Wang, Xiaofeng Liu, Yuhan Zhang, Runlin Z. Ma, Feng Wang\*

\*Corresponding author. Email: [wangfeng@ibp.ac.cn](mailto:wangfeng@ibp.ac.cn)

Published 1 April 2020, *Sci. Adv.* **6**, eaaz7825 (2020)  
DOI: [10.1126/sciadv.aaz7825](https://doi.org/10.1126/sciadv.aaz7825)

#### **This PDF file includes:**

Supplementary Text  
Figs. S1 to S23  
Tables S1 to S5

## Supplementary Text

### **Conventional phage panning protocol**

Conventional scFv-displayed phage panning was carried out using a procedure similar to the published works. Briefly, the proteins coated on a 96-well plate and incubated at 4 °C overnight. The coated wells were then washed with 0.05% DPBST, blocked with DPBST containing 4% (w/v) nonfat powdered milk, and incubated with a phage library. Following extensive wash with DPBST, 105 µl 1.75 µg/ml trypsin was added in each well to digest for 15 min at room temperature to release bound phages. The phage titer was determined by infecting 3 ml *E. coli* XL1-Blue with 10 µl of series of 1:10 diluted phages, and plated on 2×YT solid medium with Amp/Tet/10% Glucose (m/v). The phage infected XL1-blue was cultured and used to produce phages for the next round of panning.

### **Generation of secondary antibody phage library by random mutagenesis**

Random mutagenesis was performed as previously described. Briefly, a secondary phage library was constructed by GeneMorph II EZClone Domain Mutagenesis Kit (Agilent Technologies, 200552) according to manufacturer's instructions on the original output clone hC5a-35 template. Randomly mutated scFv DNA fragment (*Sfi* I digested) was ligated into the *Sfi* I linearized phagemid vector and transformed *E. coli* XL1-Blue strain. The library was packaged into multivalent scFv-pIII phages in the help of hyperphage.

### **Binding affinity measurement by surface plasmon resonance (SPR) method**

scFv-Fc proteins were immobilized onto the four individual flow cells in the CM5 sensor chip by a standard coupling protocol using Biacore T100. Briefly, the antigens were 2-fold serially diluted with DPBST, respectively. To measure the binding kinetics, the antigen and a buffer blank for baseline subtraction were sequentially injected, with a regeneration step inserted between each cycle. The scFv-Fc surface was regenerated with two 15-s pulses of glycine (pH 2.0). The binding interactions were monitored over a 60s association period and a 60s dissociation period (running buffer only). The binding kinetics curves were processed by Biacore software.

### **Primers (5'-3') used for cloning of constructs of antigens and antibodies**

IL1β primers for WT and pBpa mutant:

IL1β-WT-F: AGAAGGAGATATAACCATGGCGCCTGTGCGGAGCC

IL1β-WT-R: GGTGGTGGTGGTGGCTCGAGTCAATGGTGATGGTGA

2TAG-F: TAAGAAGGAGATATAACCATGTAGCCTGTGCGGAGCCTG

7TAG-F: TAAGAAGGAGATATAACCATGGCGCCTGTGCGGTAGCTGAACTGTACC

63TAG-F: CATTGGGCCTTTAGGAAAAGAATC

63TAG-R: GATTCTTTTCCTAAAGGCCCAATG

64TAG-F: TGGGCCTTAAGTAGAAGAATCTGT



Primers for Canakinumab or Gevokizumab IgG:

Canakinumab-HC-F:

CTGAGATCACCGGCGAAGGAGGGCCACCATGGACATGCGAGTTCCTGCCCAACTGC  
TTG

Canakinumab-HC-R:

CATCAATGTATCTTATCATGTCTGGCCAGCTAGCACTTATCATTTACCCGGAGACAG  
GGAG

Canakinumab-LC-F:

CTGAGATCACCGGCGAAGGAGGGCCACCATGGAGACGCCCGCTCAGTTGTTGTTTCT  
GCTTC

Canakinumab-LC-R:

TCTTATCATGTCTGGCCAGCTAGCACTTATCAACATTCACCTCGGTTGAATGACTTG

Gevokizumab-HC-F:

GATCACCGGCGAAGGAGGGCCACCATGGACATGCGAGTTCCTGCCCAACTGC

Gevokizumab-HC-R:

CATCAATGTATCTTATCATGTCTGGCCAGCTAGCACTTATCATTTACCCGGAGACAG  
GGAG

Gevokizumab-LC-F:

CTGAGATCACCGGCGAAGGAGGGCCACCATGGACATGCGAGTTCCTGCCCAACTGC  
TTG

Gevokizumab-LC-R:

GTCCAAACTCATCAATGTATCTTATCATGTCTGGCCAGCTAGCACTTATCAACACTC

Primers for scFv-Fc fusion proteins:

E02-scFv-Fc-F: ATTCGGCGGCCAGGCGGCCGATATTCAGATGACCCAGAG

E02-scFv-Fc-R: GATGCCAGGCCGGCCTGGCCACTAGTGAGGGTTGGGGCGG

64UV63-scFv-Fc-F: AATTCGGCGGCCAGGCGGCCGAGCTCACACTCACGCAGTCT

64UV63-scFv-Fc-R: AGATGCCAGGCCGGCCTGGCCACTAGTGAGGGTTGGGGCGGA

Primers for phage sequencing:

pSEX-pF: TTCCGGCTCGTATGTTGTGT

pSEX-pR: ACAACGCCTGTAGCATTCCA

## Sequences

### **IL1 $\beta$ WT with 6 $\times$ His tag**

Amino acid sequence:

APVRSLNCTLRDSQQKSLVMSGPYELKALHLQGQDMEQQVVFSSMSFVQGEESNDKIPV  
ALGLKEKNLYLSCVLKDDKPTLQLESVDPKNYPKKKMEKRFFVFNKIEINNKLFEFESAQF  
PNWYISTSQAENMPVFLGGTKGGQDITDFTMQFVSSLVPRGSHHHHHH

### **hC5a WT with 6 $\times$ His tag**

Amino acid sequence:

TLQKKIEEIAAKYKHSVVKCCYDGACVNNDTCEQRAARISLGPRCIKAFTECCVVAS  
QLRANISHKDMQLGRLEHHHHHHH

### **Canakinumab scFv**

amino acid sequence:

EIVLTQSPDFQSVTPKEKVTITCRASQSIGSSLHWYQQKPDQSPKLLIKYASQSFSGVPSRF  
SGSGSGTDFTLTINSLEAEDAAAYYCHQSSSLPFTFGPGTKVDIKGGSSRSSSSGGGGSGG  
GGEVQLVESGGGVVQPGRSLRLSCAASGFTFSVYGMNWVRQAPGKGLEWVAIIWYDG  
DNQYYADSVKGRFTISRDNKNTLYLQMNGLAEDTAVYYCARDLRTGPFDYWGQGT  
LTVSS

### **Gevokizumab scFv**

Amino acid sequence:

DIQMTQSTSSLSASVGDRVTITCRASQDISNYLSWYQQKPGKAVKLLIYYTSKLGSGVPS  
RFSGSGSGTDYTLTISSLQEDFATYFCLQGKMLPWTFGQGTKLEIKGGSSRSSSSGGGG  
SGGGGQVQLQESGPGLVKPSQTLSTCSFSGFSLSTSGMGVGVWIRQPSGKGLEWLAHIW  
WDGDESYNPSLKSRLTISKDTSKNQVSLKITSVTAADTAVYFCARNRYDPPWFVDWGQ  
GTLTVSS

### **Phage hC5a-35 scFv**

Amino acid sequence:

DIQMTQSPSSLSASVGDRVTITCQASQDISNYLNWYQQKPGKAPKLLIYDASNLETGVPS  
RFSGSGSGTDFTFIRSLQPEDIATYYCQQYDNLPPWTFGQGTKVEIKGGSSRSSSSGGGG  
SGGGGEVQLVESGGGLVEPGRSLRLSCTASGYTFGDYAMSWFRQAPGKDLEWVGFIRS  
KAYGGTTEYAASVKGRFTISRDDSKSIAYLQMNSLKTEDTAVYYCTRAGNDDQYFDYW  
GQGTQVTVSS

### **Phage E02 scFv**

Amino acid sequence:

DIQMTQSPSSLSASVGDRVTITCQASQDISNYLNWYQQKPGKAPKLLIYDASNLETGVPS  
RFSGSGSGTDFTFIRSLQPEDIATYYCQQYDNLPPWTFGQGTKVEIKGGSSRSSSSGGGG  
SGGGGEVQLVESGGGLVEPGRSLRLSCTASGFTFGDYAMSWFRQAPGKDLEWVGFIRS  
KAYGGTTEYAASVKGRFTISRDDSKSIAYLQMNSLKTEDTAVYYCTRAGNDDQYFDYW  
GQGTQVTVSS

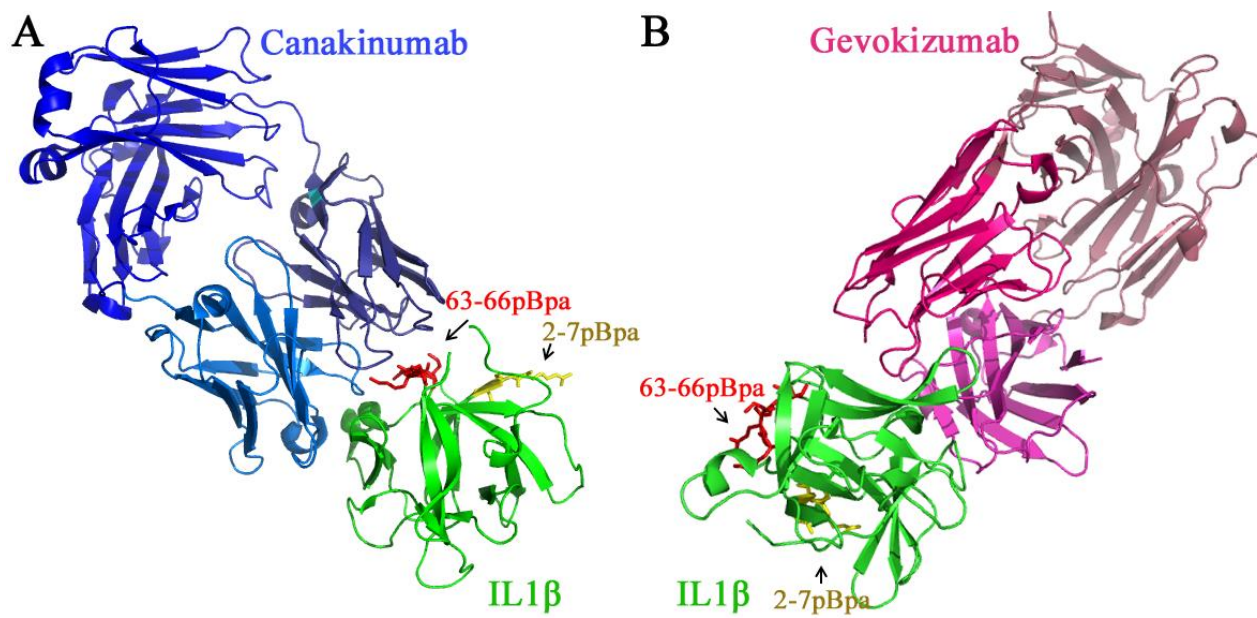


**Fig. S1. Schematic diagram of complex structures of IL1 $\beta$  bound with antibodies.**  
(A) Structure of IL1 $\beta$  bound with Canakinumab. (B) Structure of IL1 $\beta$  bound with Gevokizumab.

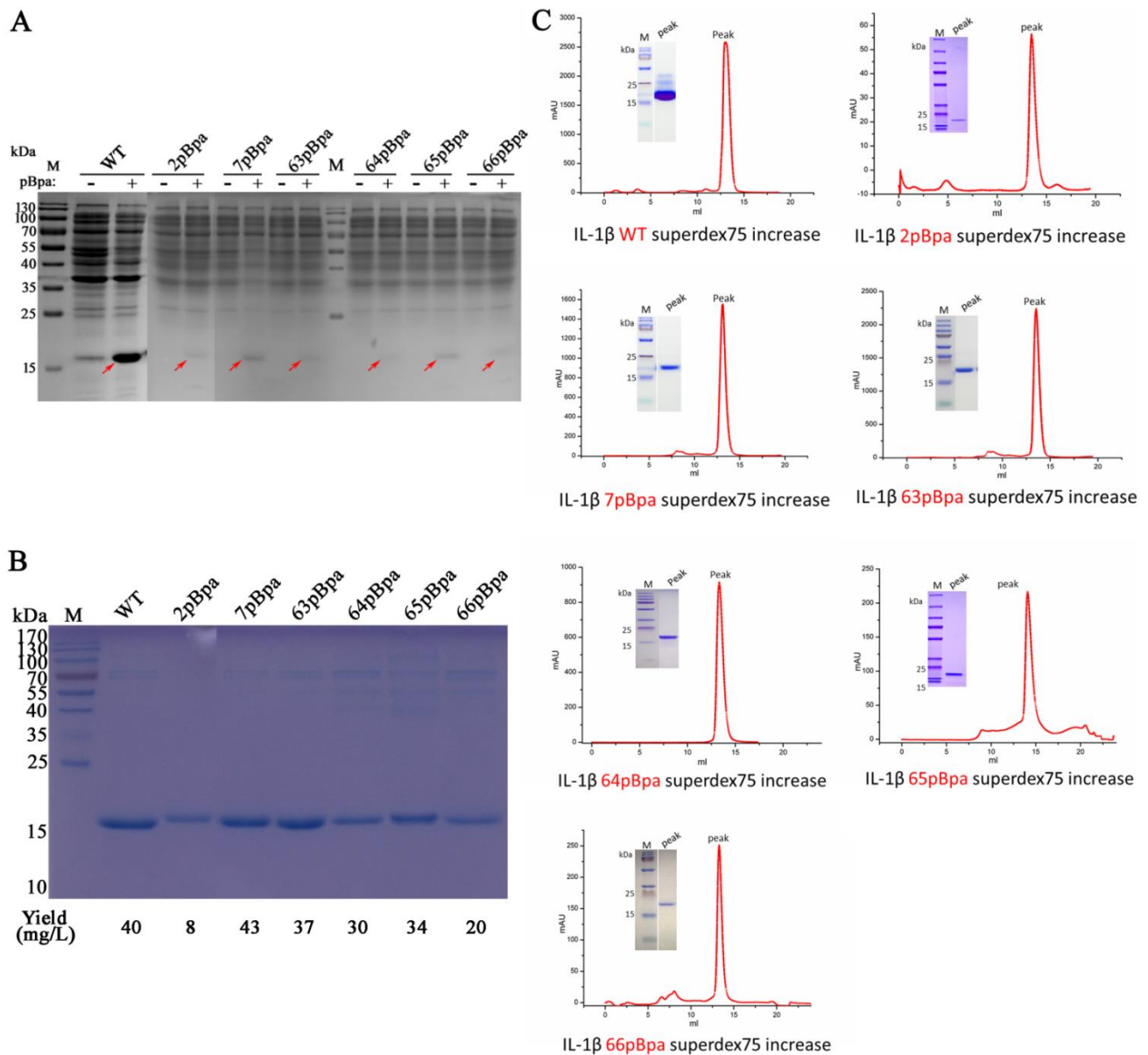
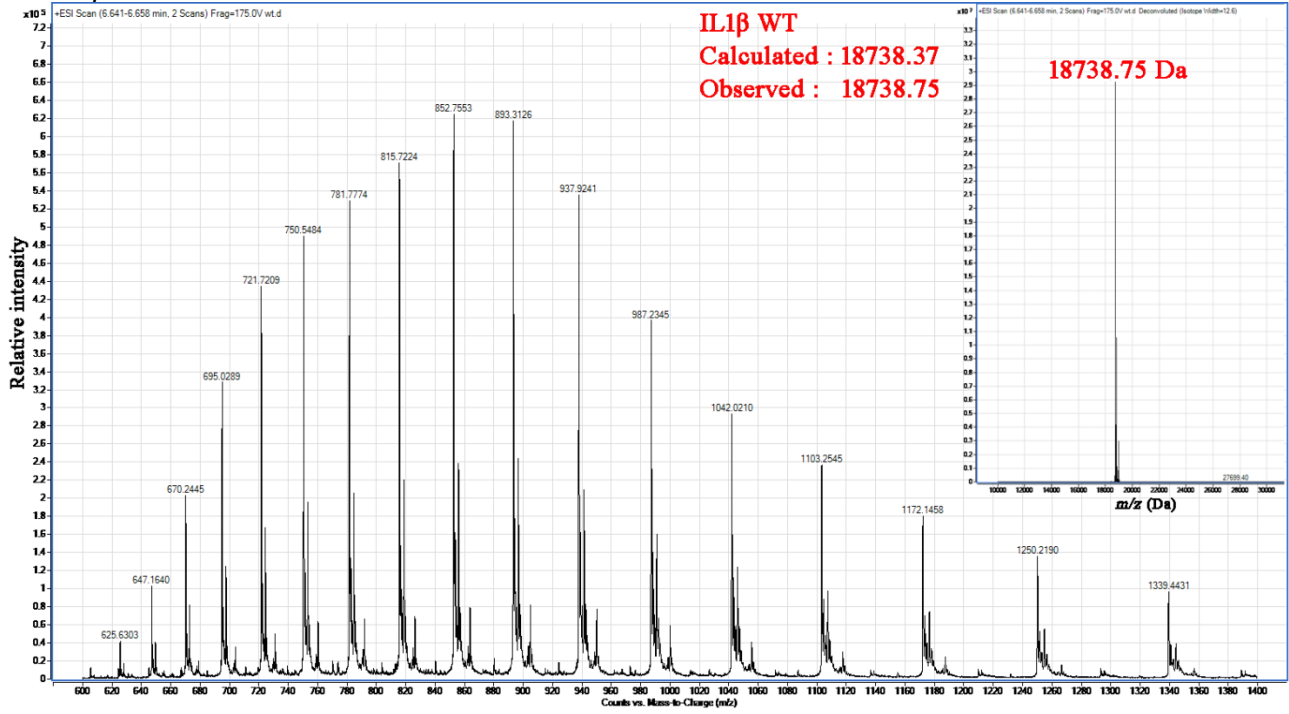


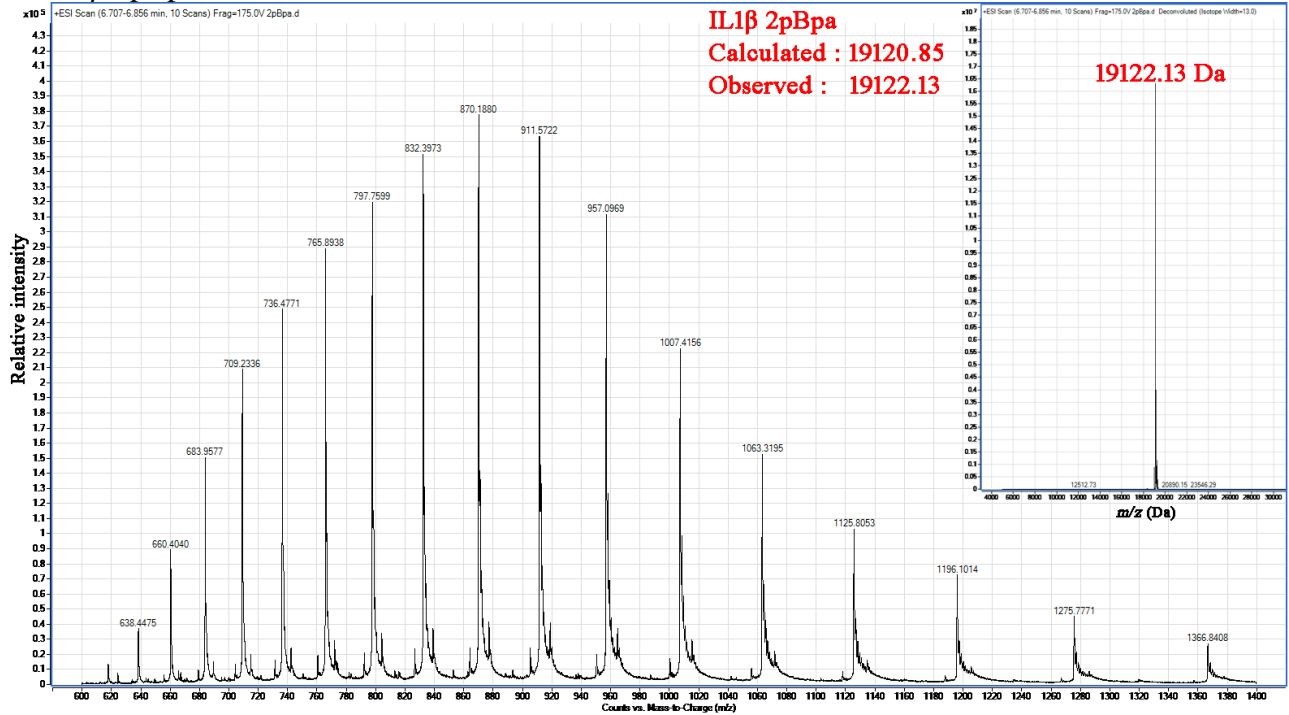
**Fig. S2. Expression and purification of wildtype and mutant IL1 $\beta$ .**

(A) Coomassie blue-stained SDS-PAGE of His tag-IL1 $\beta$  (WT and mutant) expressed in the presence (+) or absence (-) of pBpa (1mM) by *E. coli* BL21 (DE3). The red arrow indicates the expression of the full-length WT and mutant IL1 $\beta$ . (B) Coomassie blue-stained SDS-PAGE of WT and mutant IL1 $\beta$  after purification by Ni-NTA affinity chromatography. (C) WT and mutant IL1 $\beta$  purified by size-exclusion chromatography in PBS buffer.

### A IL1 $\beta$ WT Mass

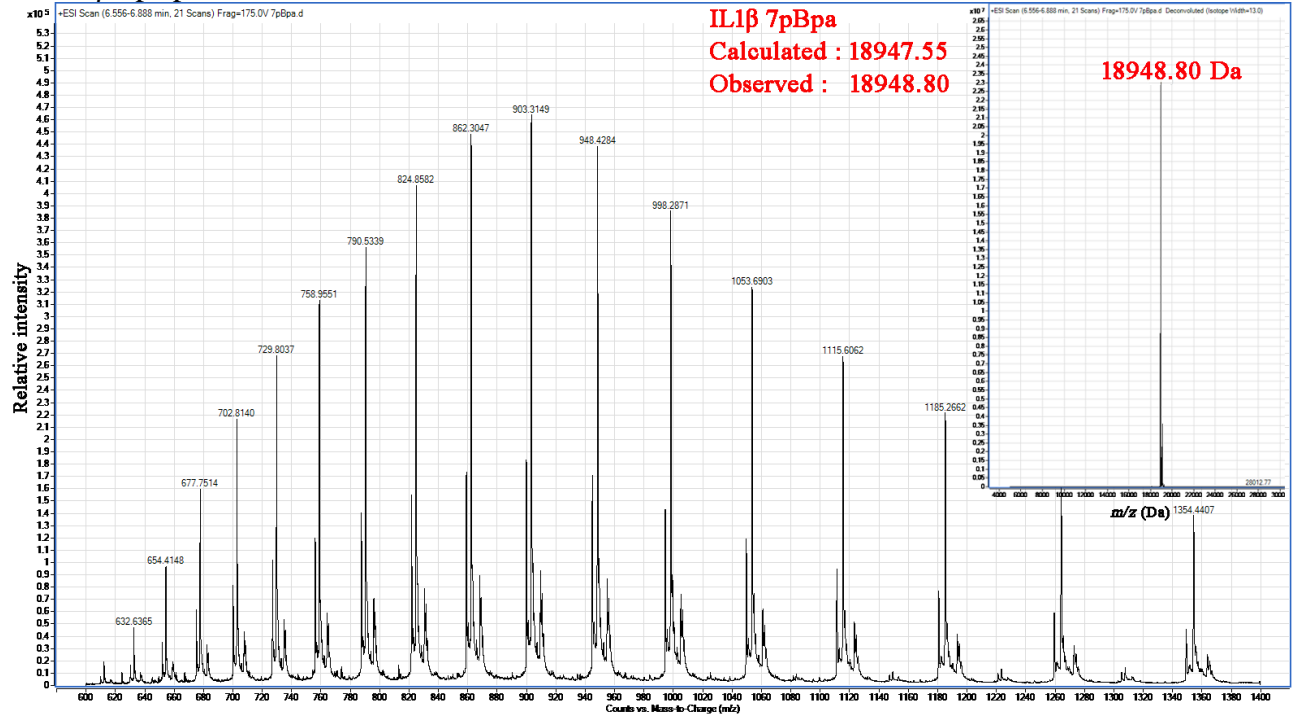


### B IL1 $\beta$ 2pBpa mutant Mass

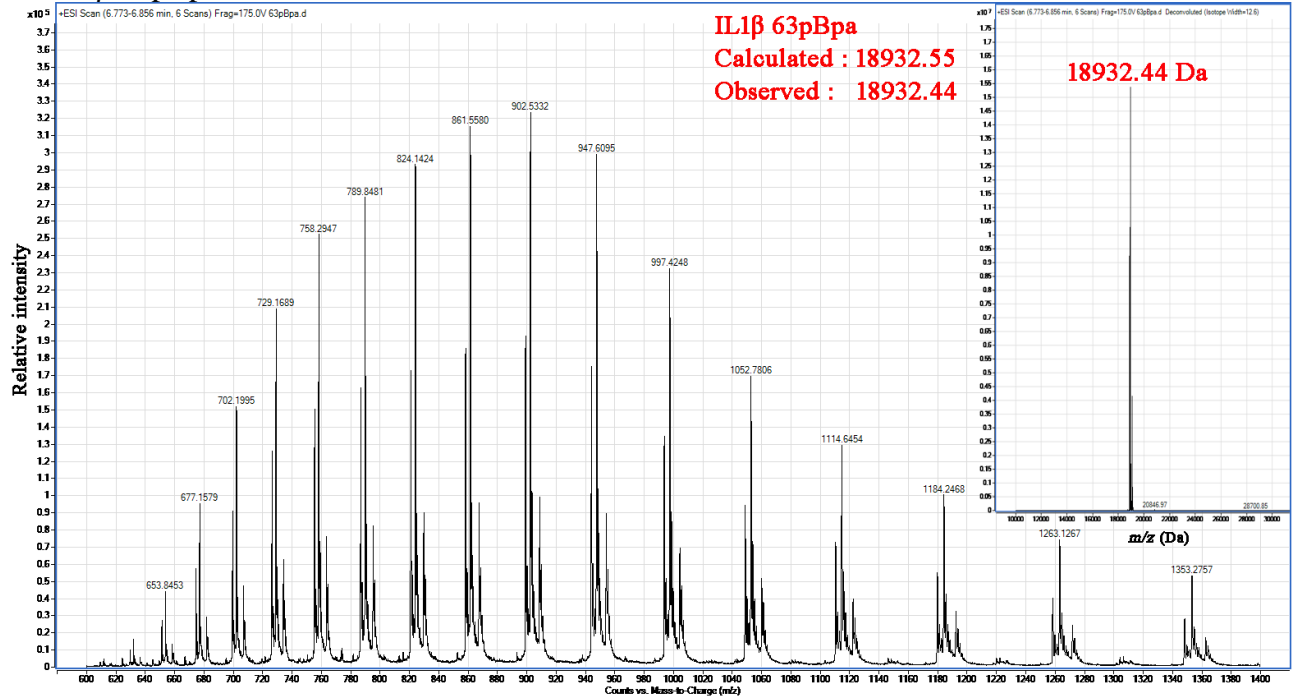




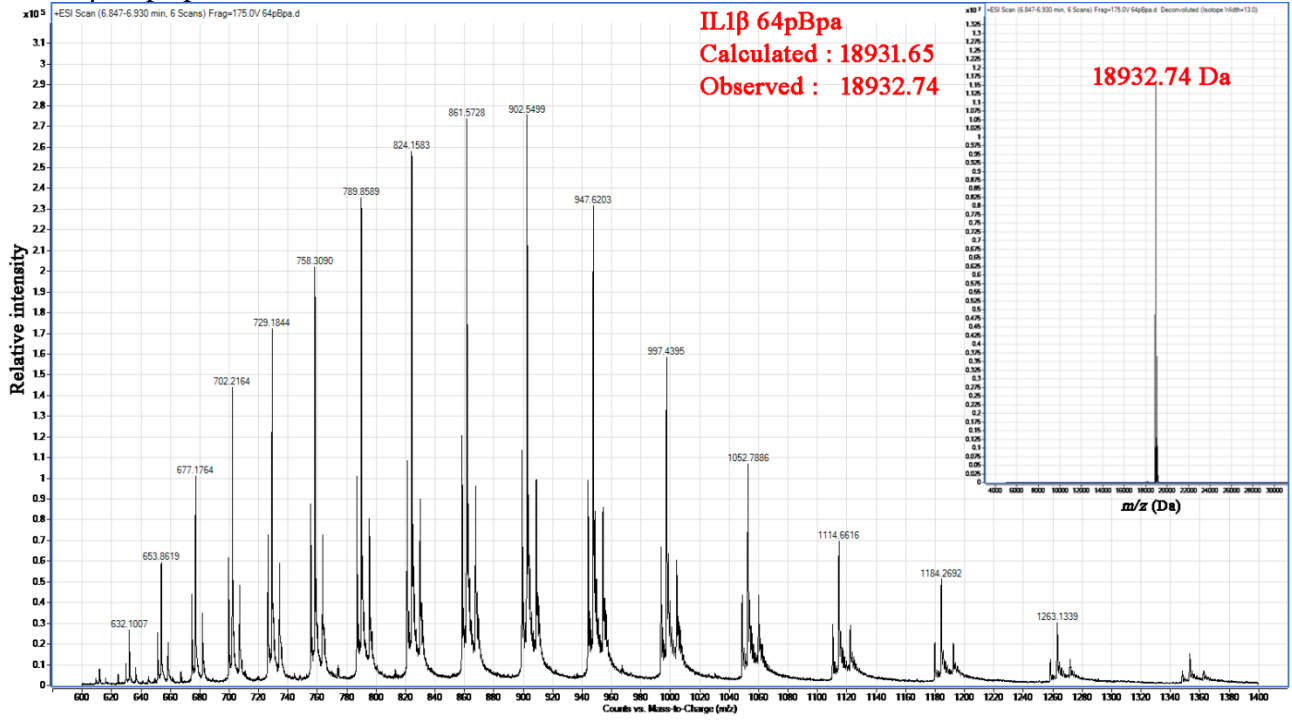
### C IL1 $\beta$ 7pBpa mutant Mass



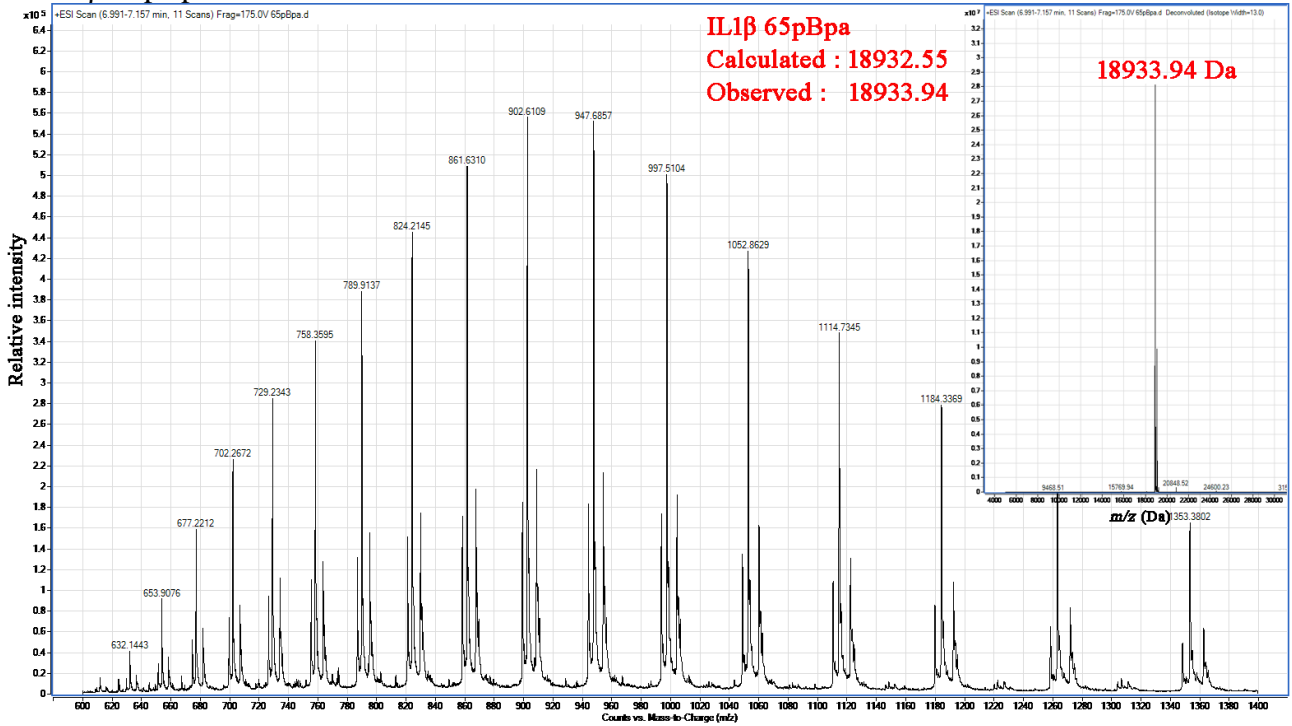
### D IL1 $\beta$ 63pBpa mutant Mass



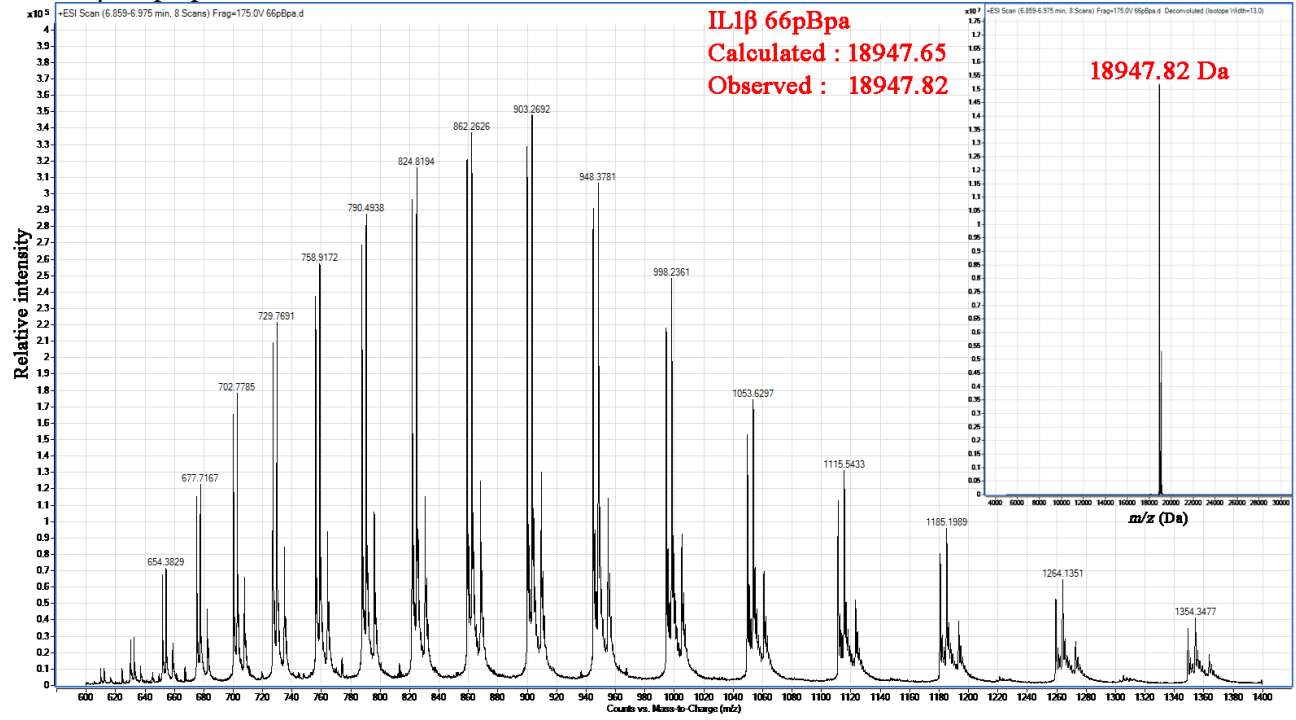
### E IL1 $\beta$ 64pBpa mutant Mass



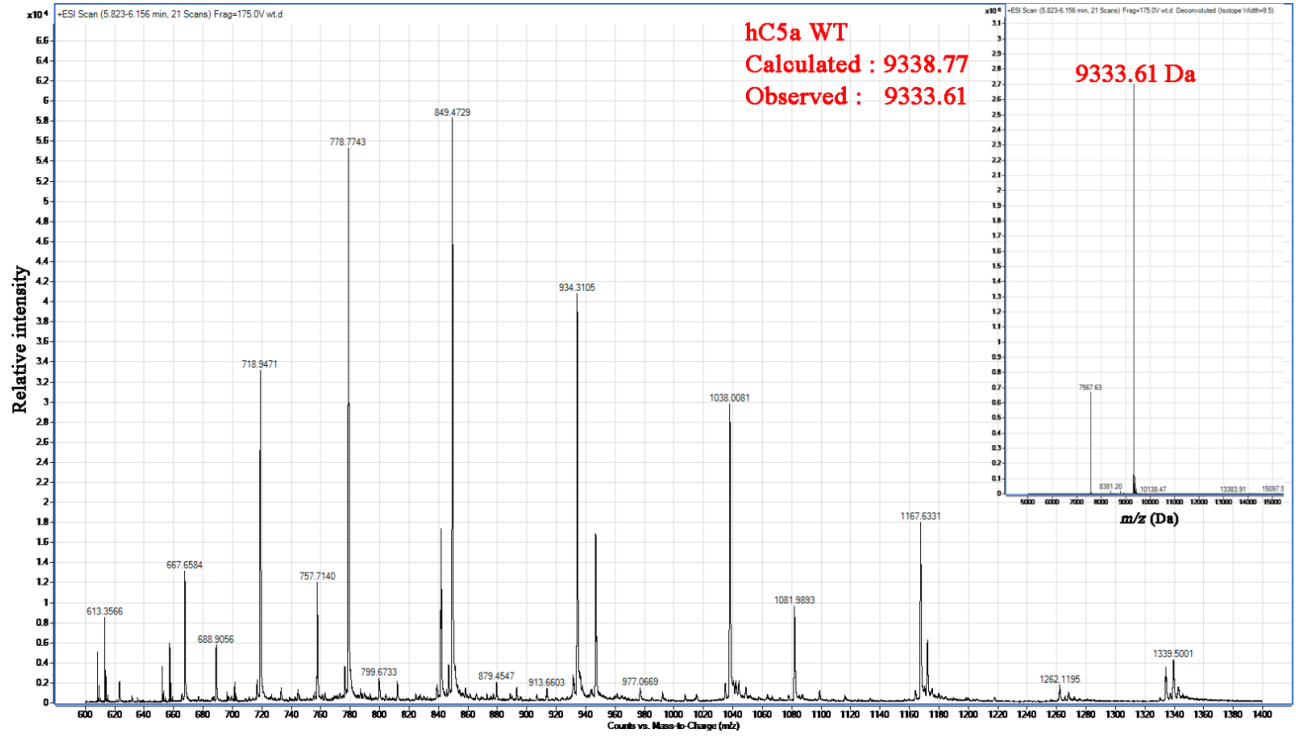
### F IL1 $\beta$ 65pBpa mutant Mass



### G IL1 $\beta$ 66pBpa mutant Mass



### H hC5a WT Mass



# I hC5a 18pBpa mutant Mass

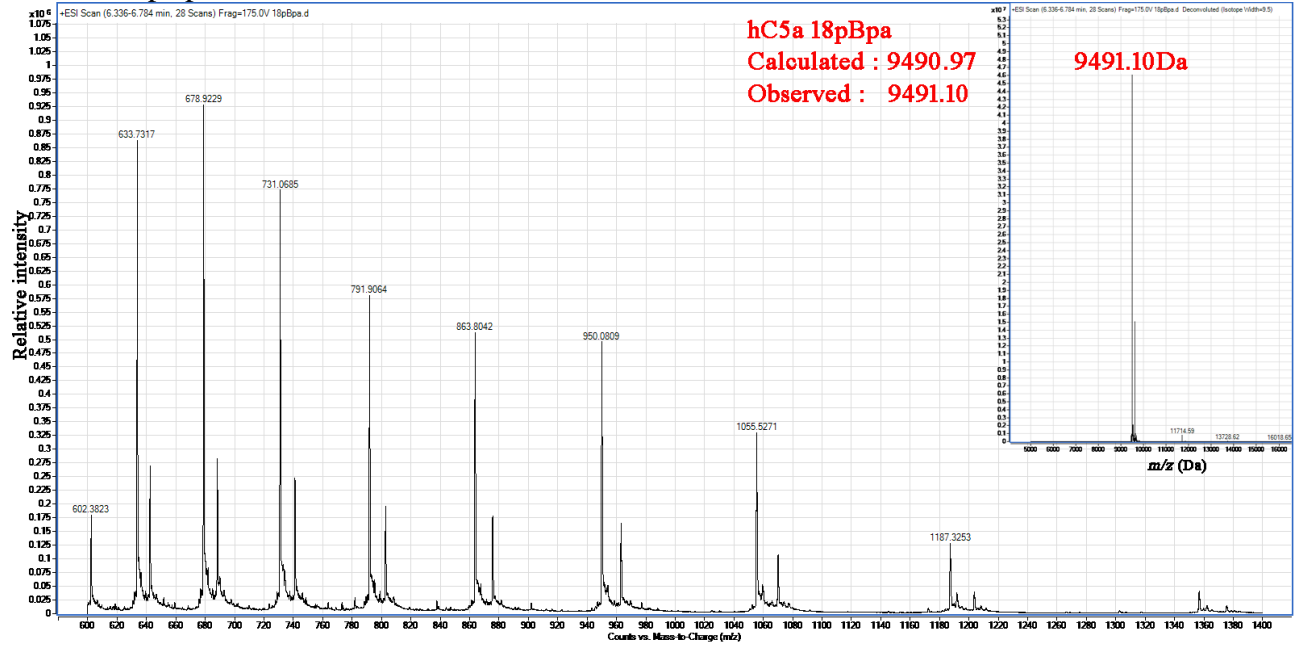
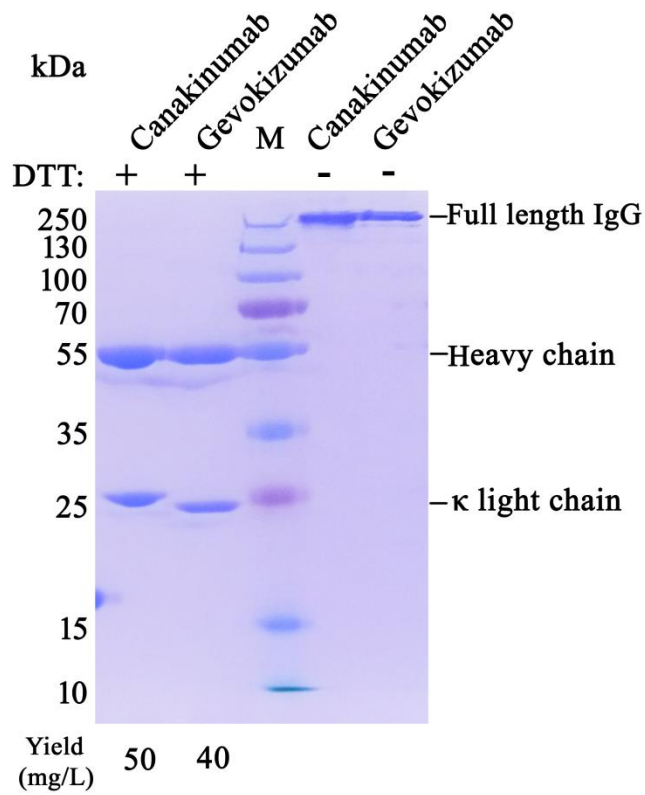
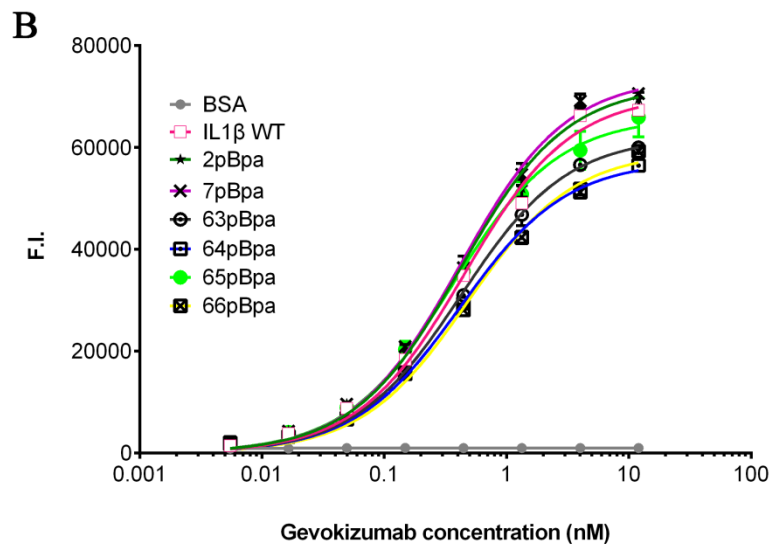
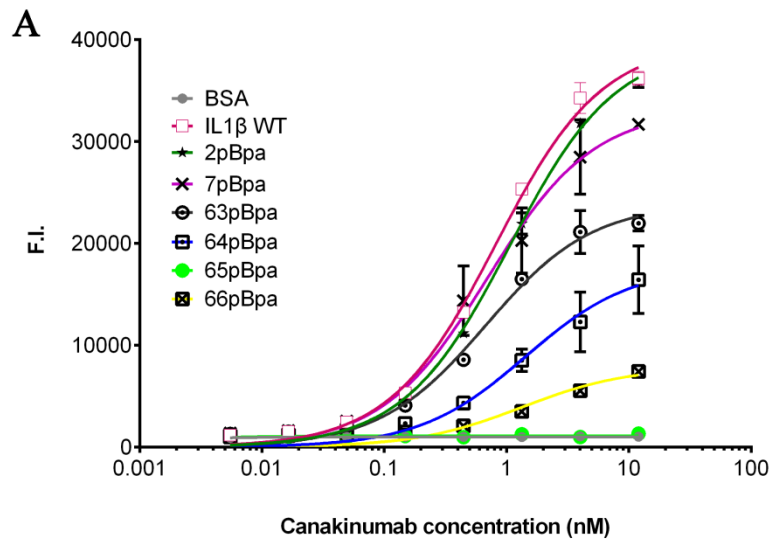


Fig. S3. ESI Q-TOF MS analysis of WT and pBpa incorporated mutants.  
Inset, mass spectrum after deconvolution.



**Fig. S4. Coomassie blue-stained SDS-PAGE of Canakinumab and Gevokizumab.** Proteins were purified by Protein-A affinity chromatography and size-exclusion chromatography.



**Fig. S5. Binding of WT and pBpa incorporated IL1 $\beta$  with Canakinumab and Gevokizumab by ELISA.**

(A) Binding of WT and mutants with Canakinumab in a concentration-dependent manner. (B) Binding of WT and mutants with Gevokizumab in a concentration-dependent manner.

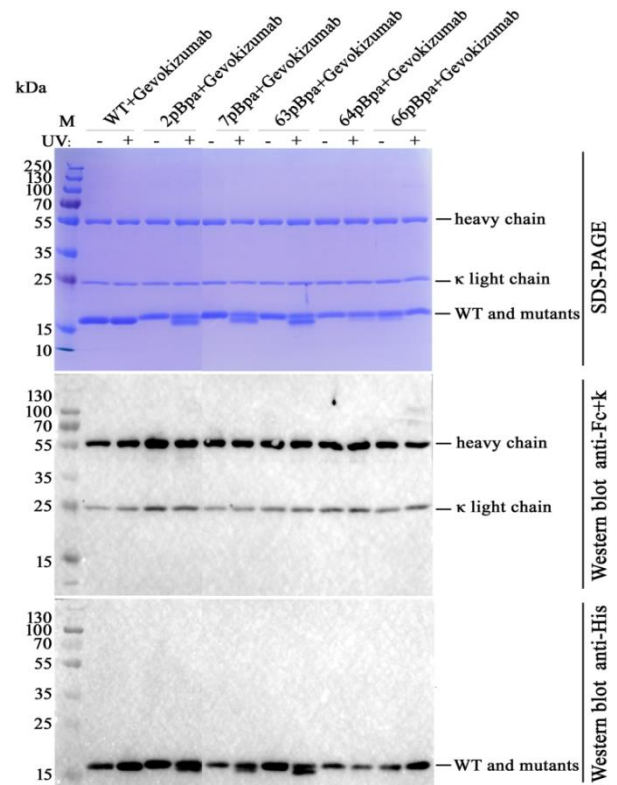
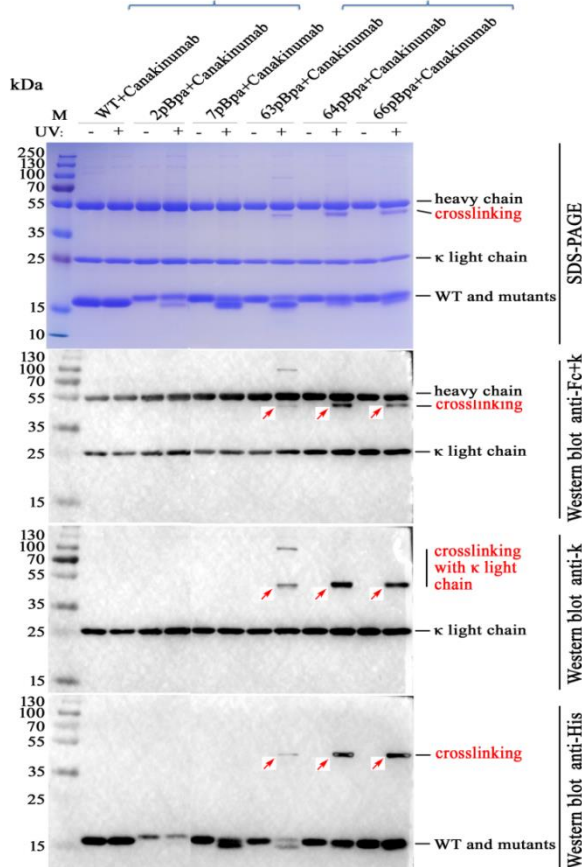
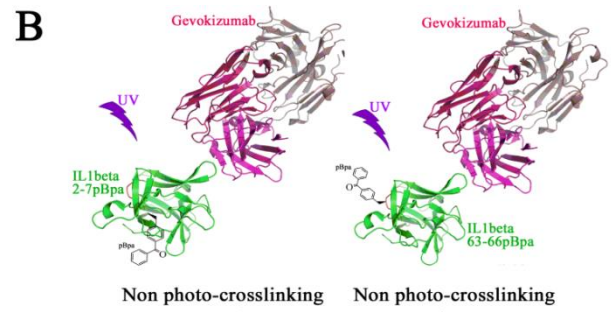
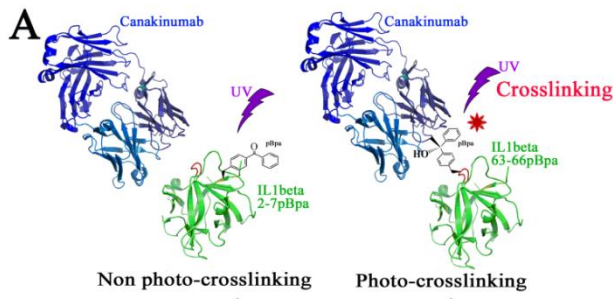


**Fig. S6. Analysis of products of IL1β and antibodies after UV irradiation.**

(A) UV induced photo-crosslinking could be observed between Canakinumab and 63pBpa, 64pBpa, 66pBpa mutants, but not wild type IL1β, 2pBpa, 7pBpa, by SDS-PAGE and Western blot using anti-His (ZSGB-BIO, TA-02) (detecting IL1β), anti-Kappa light chain and anti-human Fc HRP (SeraCare Life Sciences, 5220-0270) (detecting Canakinumab). (B) Under the same condition, photo-crosslinking could not be observed between Gevokizumab and WT and mutant IL1β.

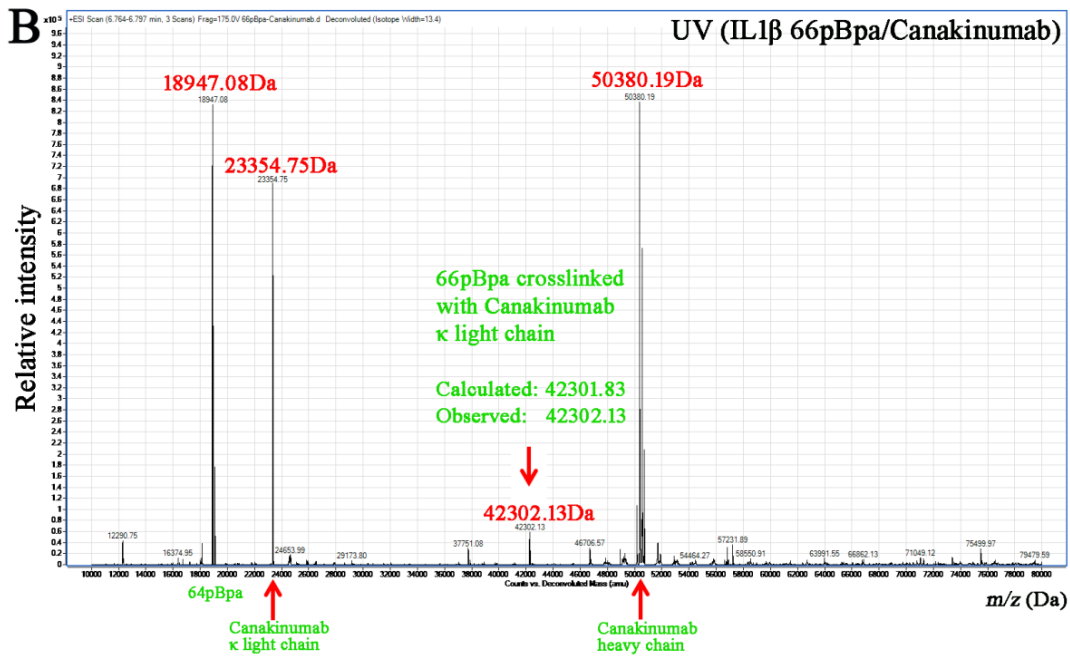
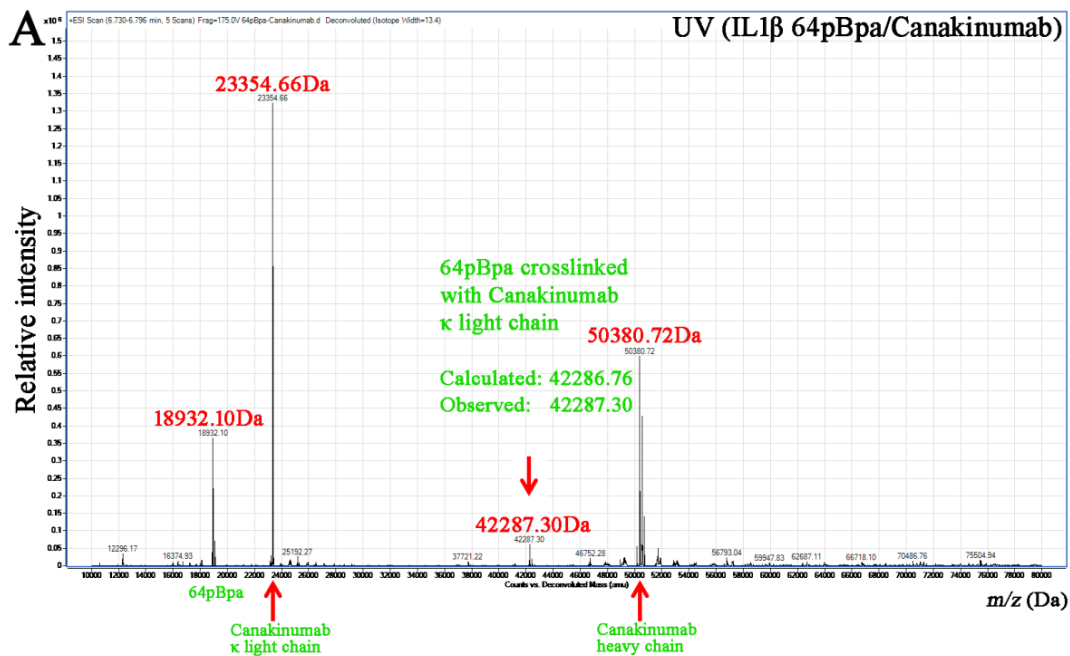


**Fig. S7. ESI Q-TOF MS analysis of products of IL1 $\beta$  and antibodies after UV irradiation.** (A) ESI Q-TOF MS analysis was performed with samples that were produced by incubating 10 $\mu$ g Canakinumab and 1 $\mu$ g 64pBpa mutant after 10-hour irradiation by 365 nm UV (6 W). (B) ESI Q-TOF MS analysis was performed with samples that were produced by incubating 20 $\mu$ g Canakinumab and 20 $\mu$ g 66pBpa mutant after 10-hour irradiation by 365 nm UV (6 W).



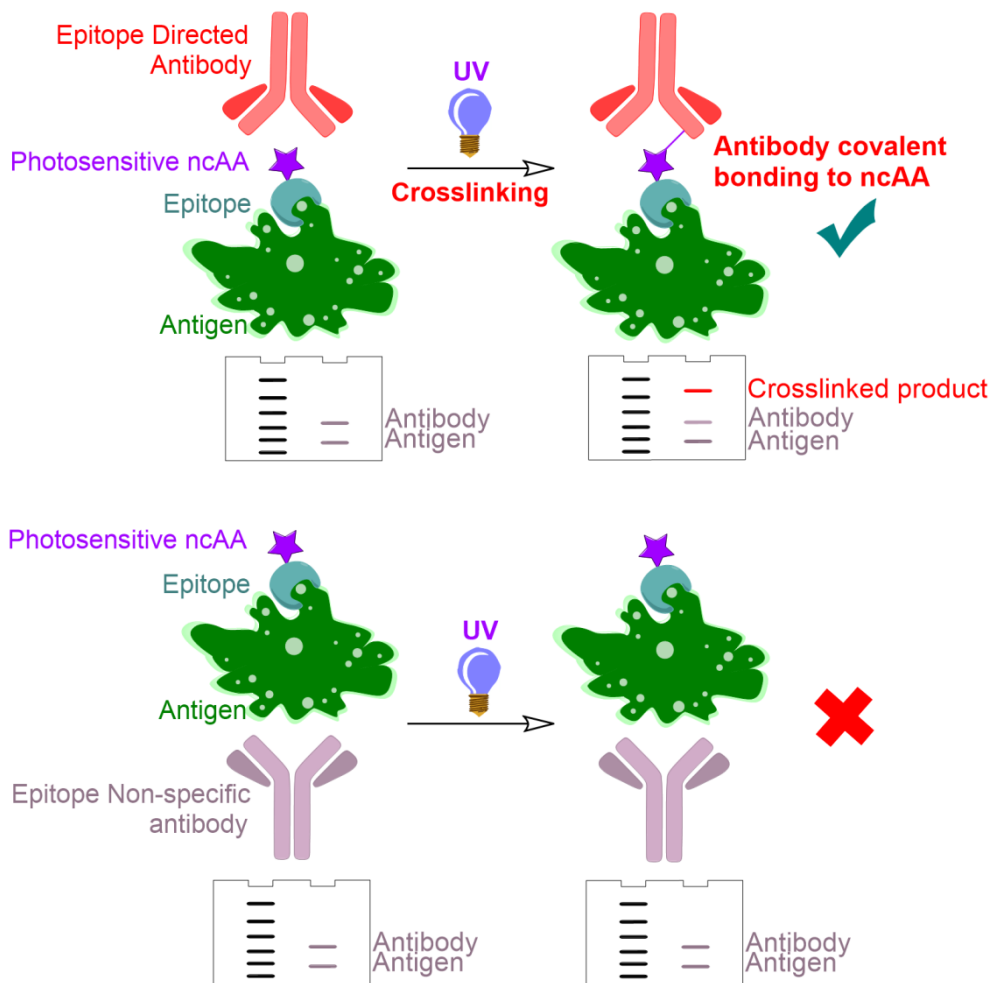


**Fig. S8. Schematic diagram of crosslinking between the antibody and photosensitive nCAA in epitope of antigen can occur after irradiation.**

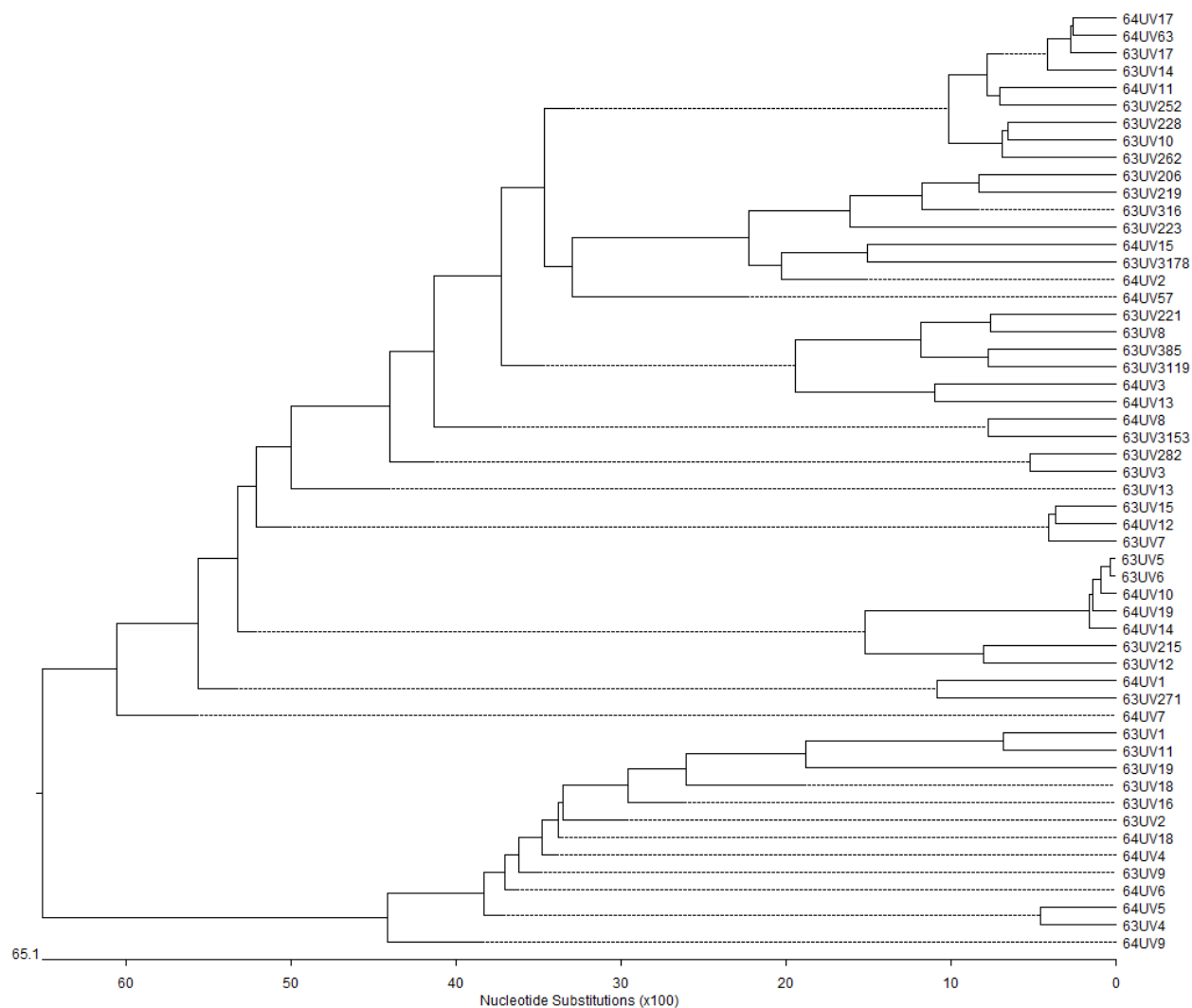


**Fig. S9. Sequence analysis of hit pools of 63pBpa and 64pBpa from epitope-directed phage library selection (n = 55).**

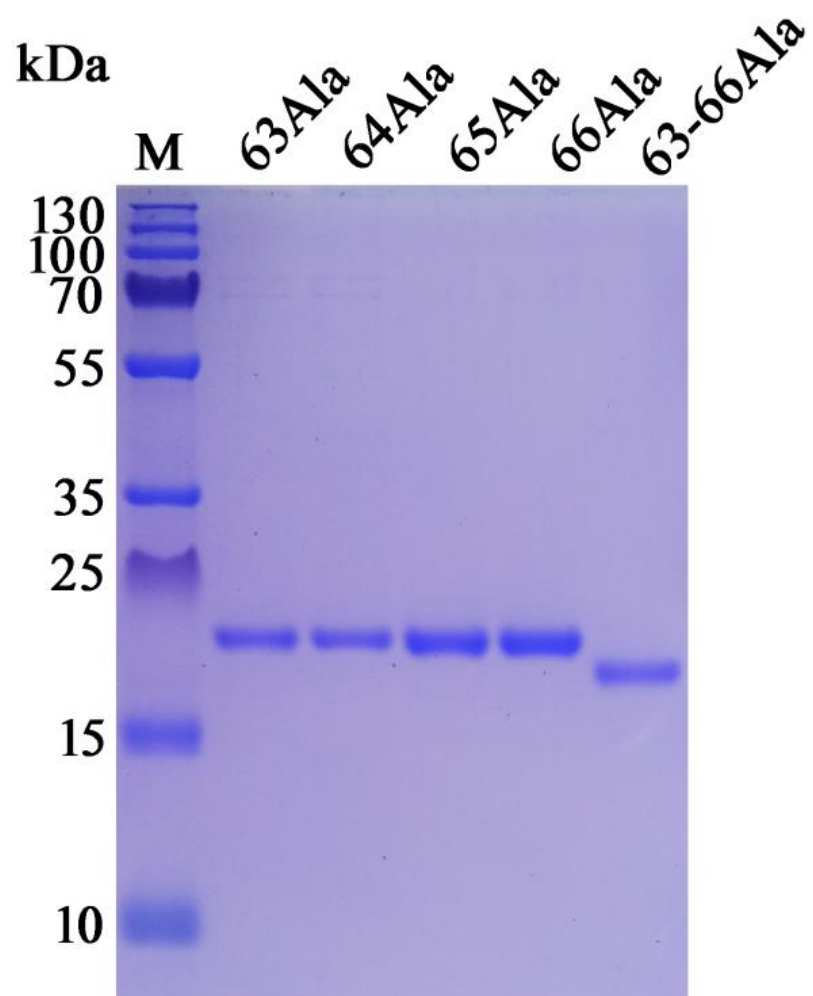


**Fig. S10.** SDS-PAGE analysis of single and quadruple alanine mutants of IL1 $\beta$  after purification.

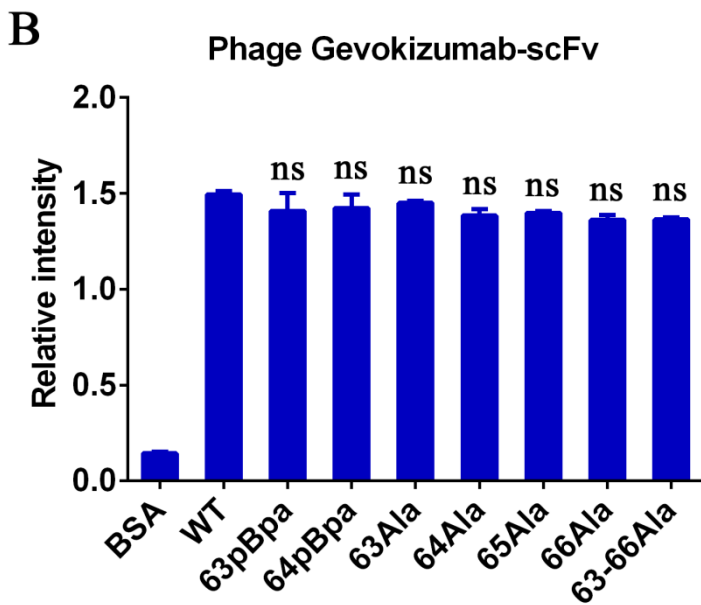
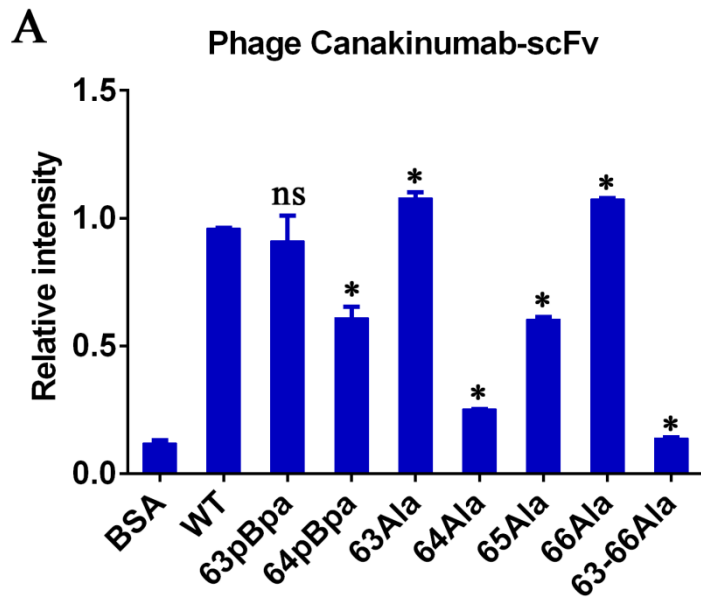


**Fig. S11. Binding of monoclonal phages of Canakinumab-scFv and Gevokizumab-scFv on WT and mutant IL1 $\beta$  analyzed by ELISA.**

The  $p$  value of WT group vs mutant groups. \* $p < 0.05$ ,  $^{ns}p \geq 0.05$ .

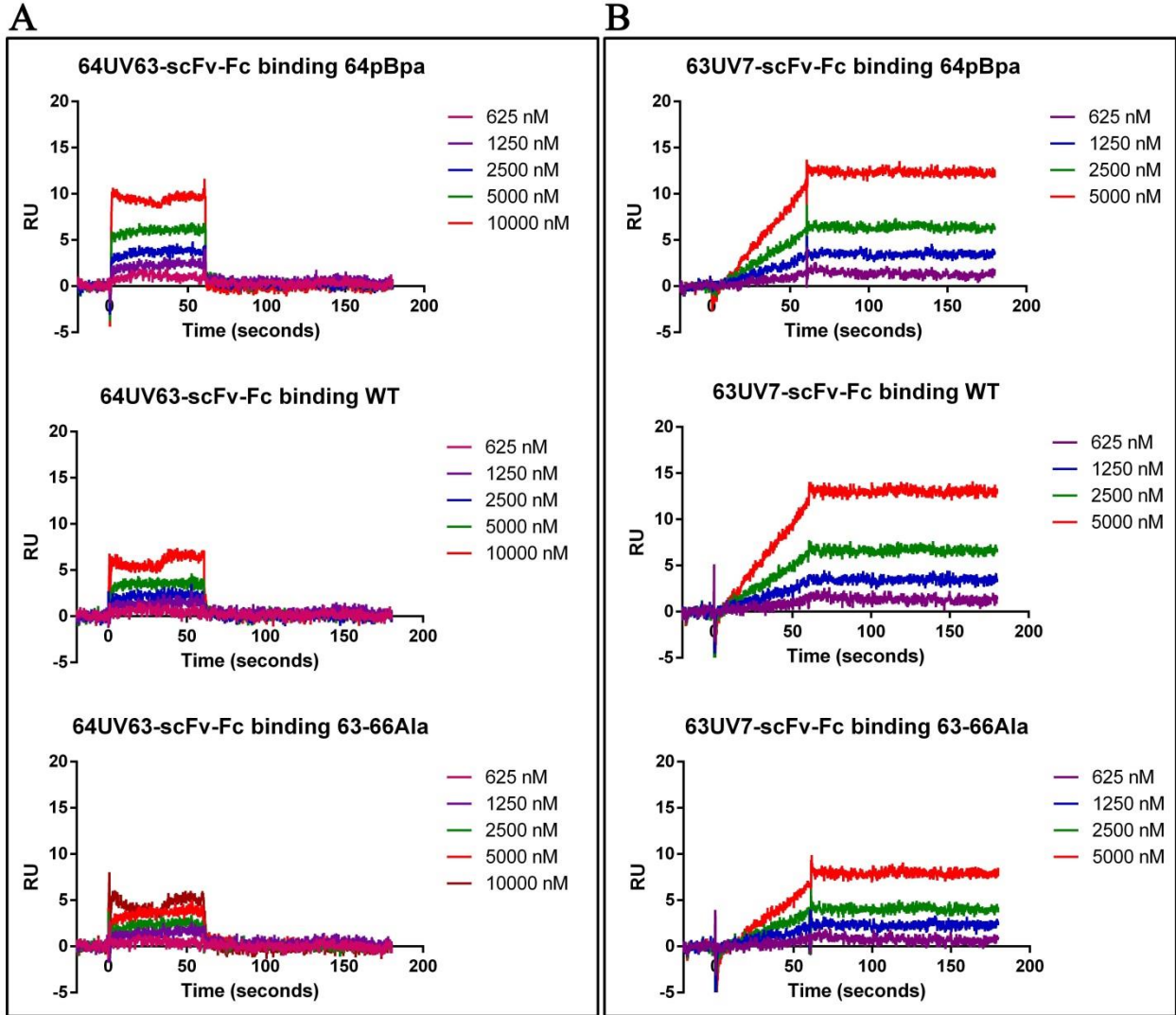


**Fig. S12. Binding affinities of 64UV63 (A) and 63UV7 (B) scFv-Fc fusion proteins against pBpa mutant, WT IL1 $\beta$  and alanine mutant, measured by Biacore T100.**

The on-rate, off-rate, and binding constant of 64UV63 could not be accurately deduced due to weak binding affinity. The  $k_a$ ,  $k_d$ , and  $K_D$  of 63UV7 on 64pBpa are 383.2 1/M.s, 1.2E-04 1/s, 3.2E-07 M, respectively, and those on WT IL1 $\beta$  are 577.8 1/M.s, 2.1E-04 1/s, 3.6E-07 M.

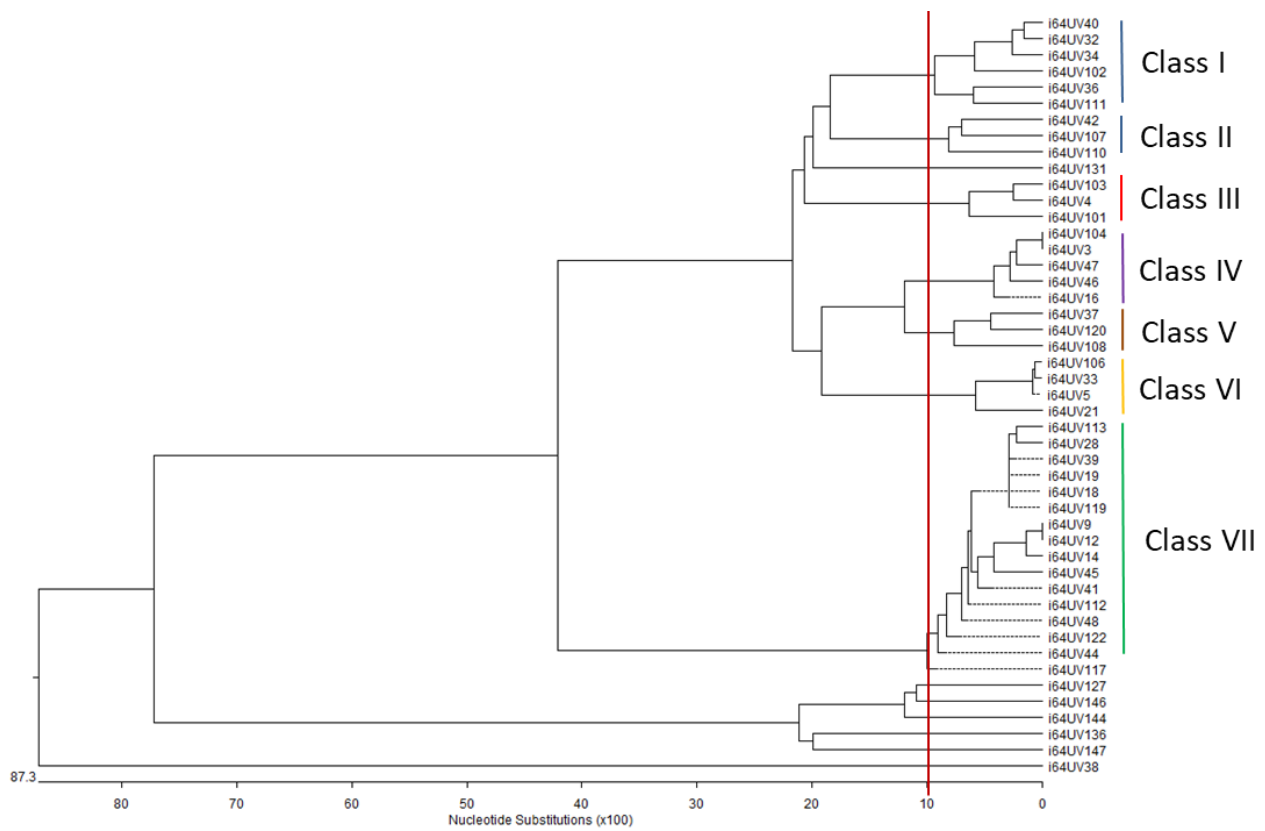


**Fig. S13. Sequence analysis of the hit pool of epitope-directed panning phage library generated from mouse immunization of IL1 $\beta$  (n = 47) against 64pBpa.**

Seven sequence clusters were identified based on homology (with at least two homologous sequences when 10x100 nucleotide substitutions cutoff was applied).

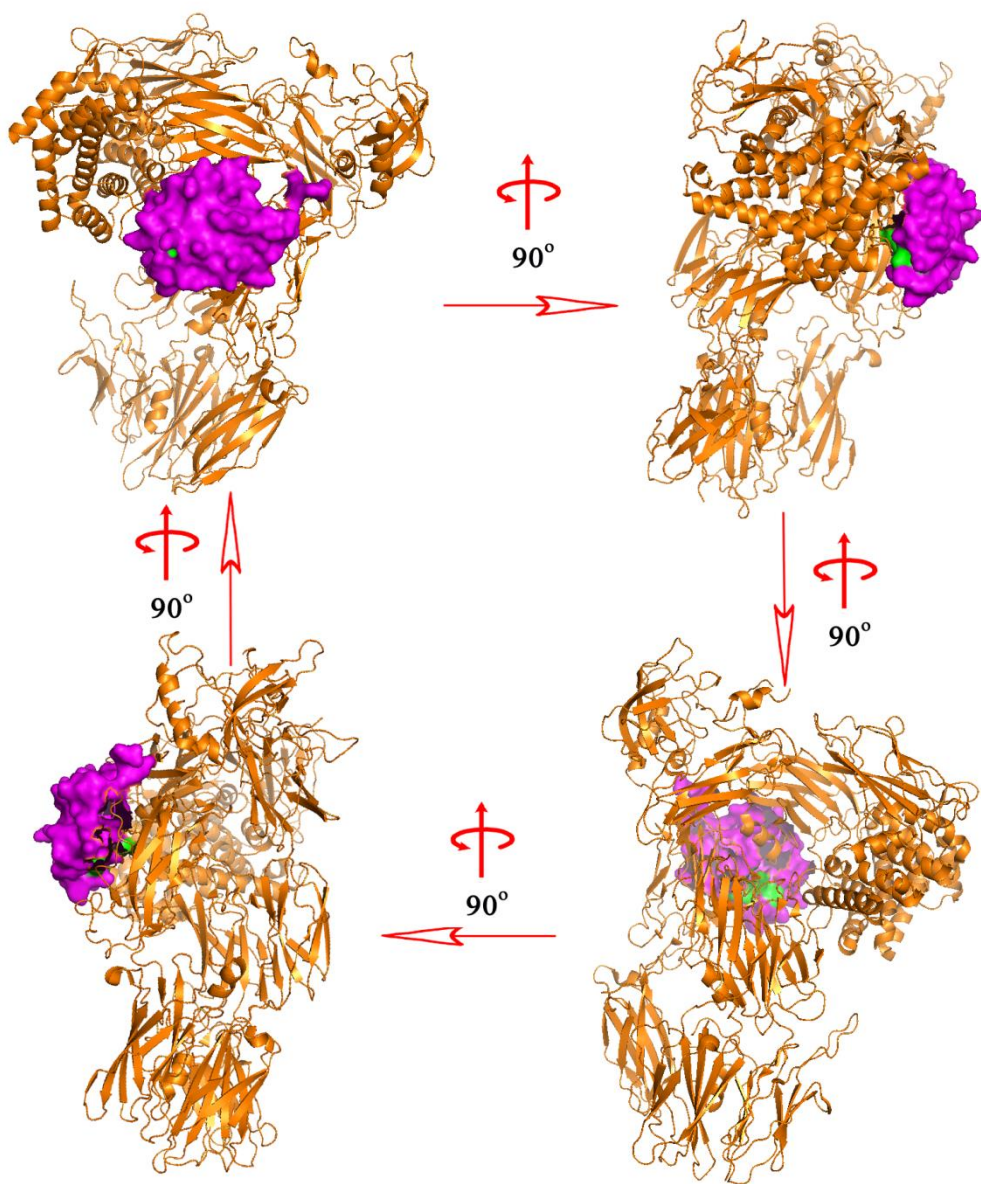


**Fig. S14. The crystal structure of hC5 in four different angles of views after rotating by 90 degrees.**

The structure of hC5 was colored in orange and the sequence region of hC5a was colored in purple. The targeted epitope of hC5a (SVVKK) is covered in the surface of hC5 (colored in green).

	1	10	20	30	40	50	60	70																																																														
<b>Human C5a</b>	M	L	Q	K	I	E	E	I	A	A	K	<u>H</u>	S	V	V	K	C	C	Y	D	G	A	C	V	N	D	E	T	C	E	Q	R	A	A	R	I	S	L	G	P	R	C	I	K	A	F	T	E	C	C	V	V	A	S	Q	L	R	A	N	I	S	H	K	D	M	Q	L	G	R	
<b>Monkey C5a</b>	L	K	K	I	E	E	I	A	A	K	K	H	F	V	V	K	C	C	Y	D	G	A	C	I	N	D	E	T	C	E	Q	R	A	A	R	I	S	V	G	P	R	C	V	K	A	F	T	E	C	C	V	V	A	S	Q	L	R	A	N	M	S	H	K	D	M	Q	L	G	R	
<b>Mouse C5a</b>	L	L	R	Q	I	E	E	Q	A	A	K	K	H	S	V	P	K	C	C	Y	D	G	A	R	V	N	F	Y	E	T	C	E	E	R	V	A	R	V	T	I	G	P	L	C	I	R	A	F	N	E	C	T	I	A	N	K	I	R	K	E	S	P	H	K	P	V	Q	L	G	R

**Fig. S15. Sequence alignment of C5a of human, monkey and mouse.**

Identical and similar residues are highlighted in black and grey, respectively. The targeted epitope is marked with an underline.



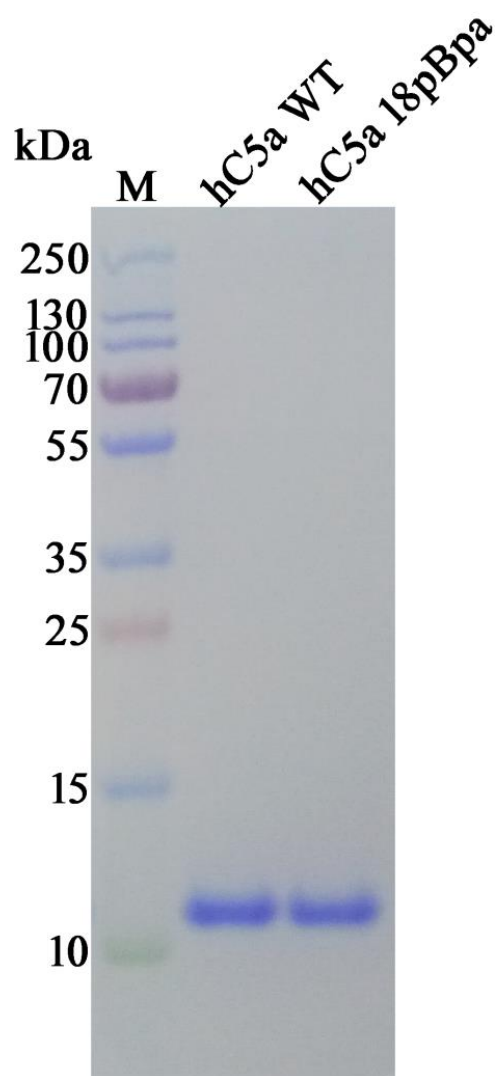


**Fig. S16. SDS-PAGE analysis of WT and pBpa incorporated mutant hC5a (18pBpa) after purification.**

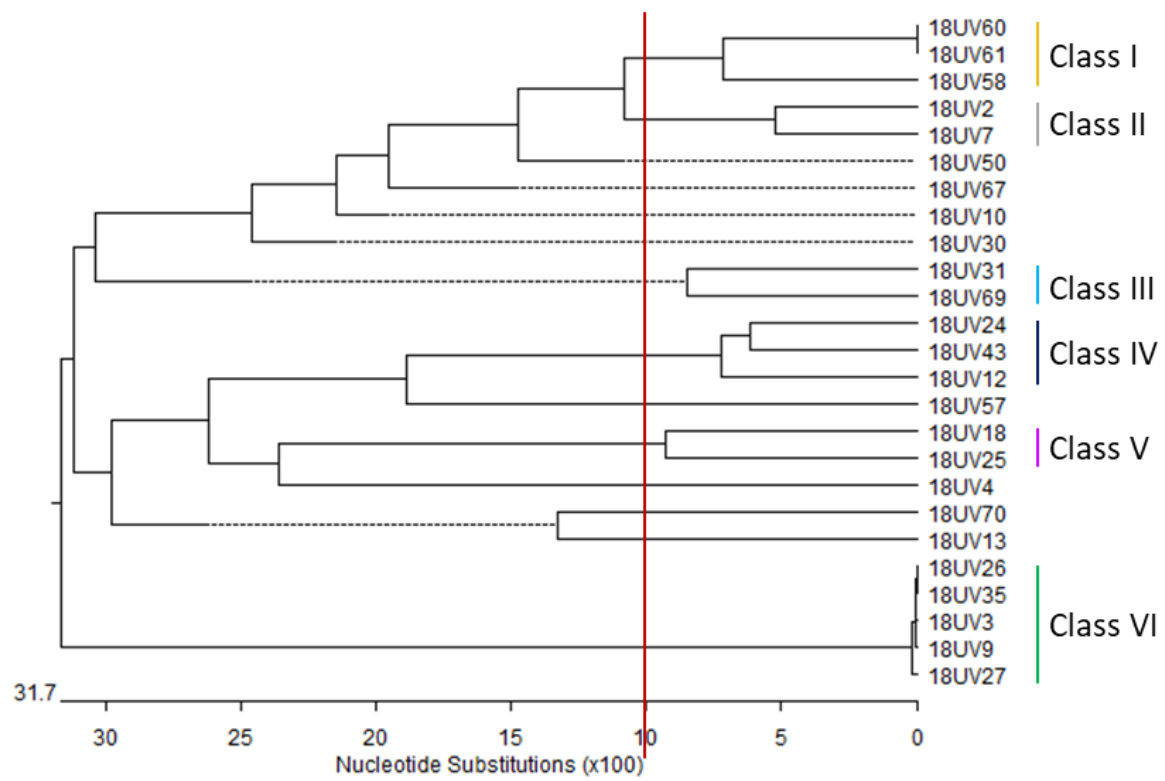


**Fig. S17. Sequence analysis of hit pool from epitope-directed panning human naïve phage library against hC5a-18pBpa.**

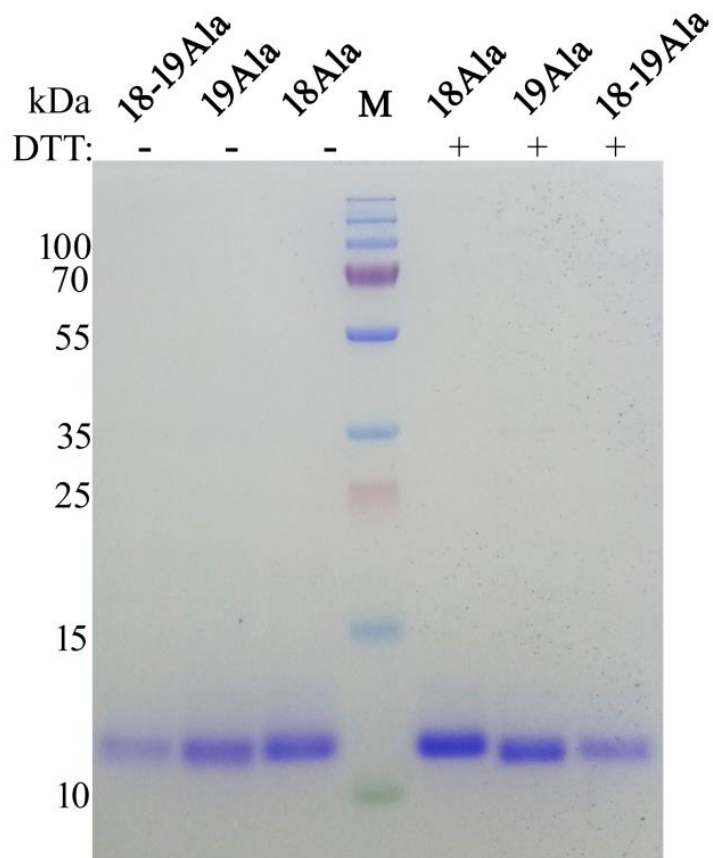


**Fig. S18. SDS-PAGE analysis of single and double alanine mutants of hC5a after purification.**

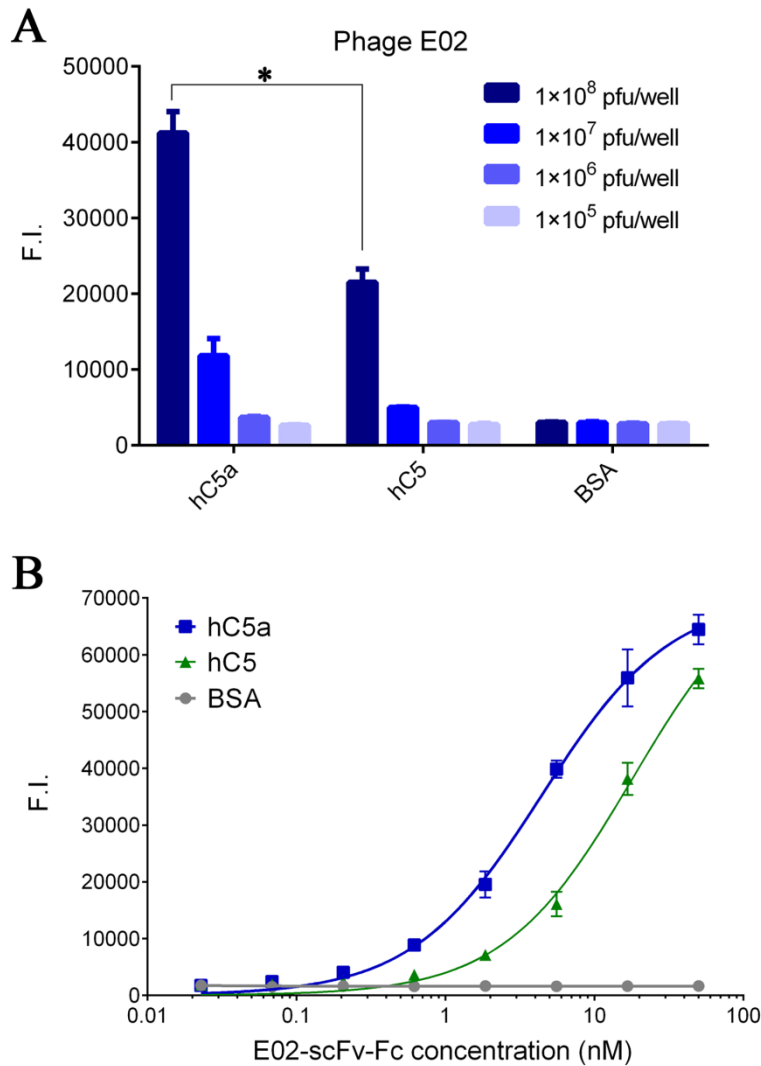


**Fig. S19. E02 scFv displayed phages and scFv-Fc fusion protein exhibited stronger binding affinity to hC5a than hC5.**

(A) Comparison of binding of E02 phages to hC5a and hC5. 100 ng/well of hC5a (Sino Biological, 10604-HNAE), hC5 (Millipore, 204888-25), and BSA were coated on plate. Phages with a series of titers were added for ELISA. Anti-M13 HRP was used as 2<sup>nd</sup> antibody and exposed with QuantaBlu (Thermo Scientific, 15169) for signal production. The *p* value of hC5a group vs hC5 group. \**p*<0.05. (B) Comparison of binding of E02-scFv-Fc to hC5a and hC5. Anti-Fc HRP (GE Healthcare, 27-9421-01) was used as 2<sup>nd</sup> antibody and exposed with QuantaBlu for signal production.

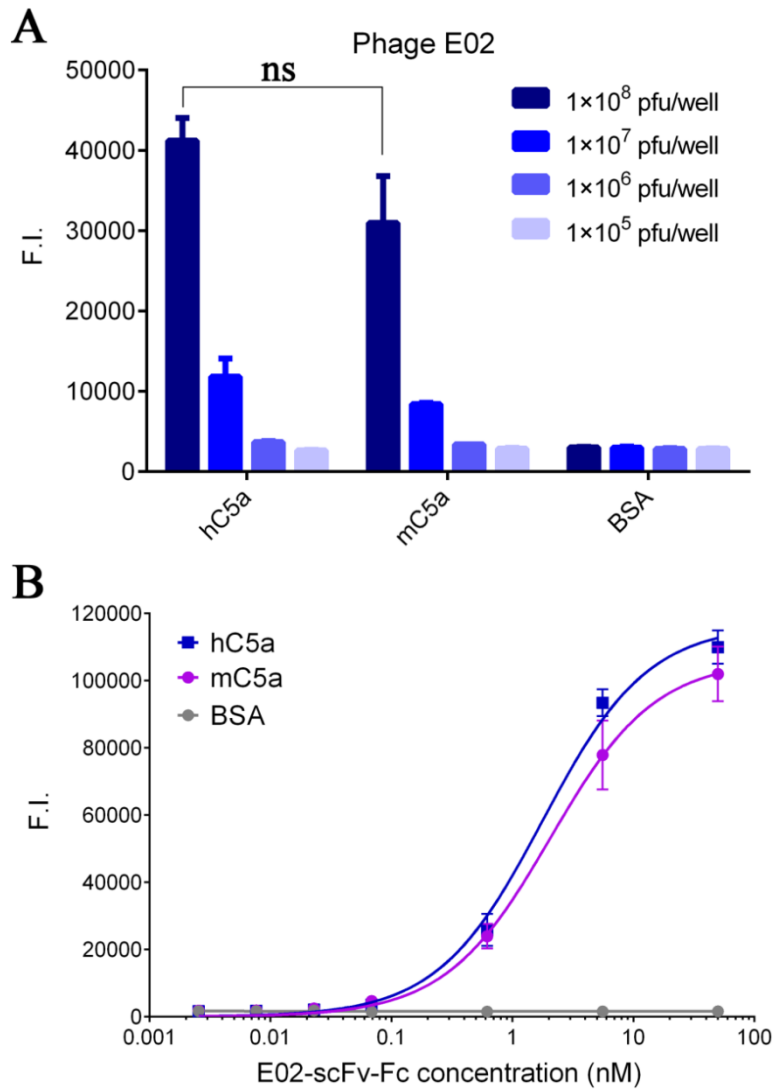


**Fig. S20. E02 scFv displayed phages and scFv-Fc fusion protein exhibited similar binding affinity to hC5a and mC5.**

(A) Comparison of binding of E02 phages to human C5a and mouse C5a. 100 ng/well of hC5a (Sino Biological, 10604-HNAE), mC5a (Novoprotein, C075-50UG), and BSA were coated on plate. Phages with a series of titers were added for ELISA. Anti-M13 HRP was used as 2<sup>nd</sup> antibody and exposed with QuantaBlu for signal production. The *p* value of hC5a group vs mC5a group. <sup>ns</sup>*p* ≥ 0.05. (B) Comparison of binding of E02-scFv-Fc to hC5a and mC5a. Anti-Fc HRP was used as 2<sup>nd</sup> antibody and exposed with QuantaBlu for signal production.

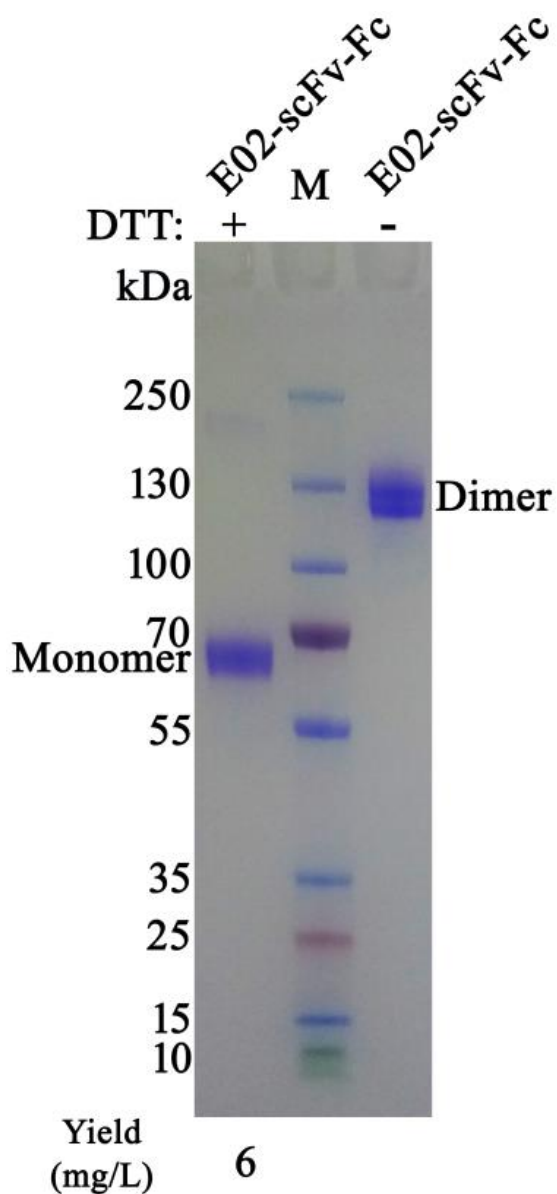


**Fig. S21. SDS-PAGE analysis of reduced and non-reduced E02-scFv-Fc fusion protein.** E02-scFv-Fc was expressed by transient transfection of 293FS cells followed by purification by Protein A and size-exclusion chromatography.

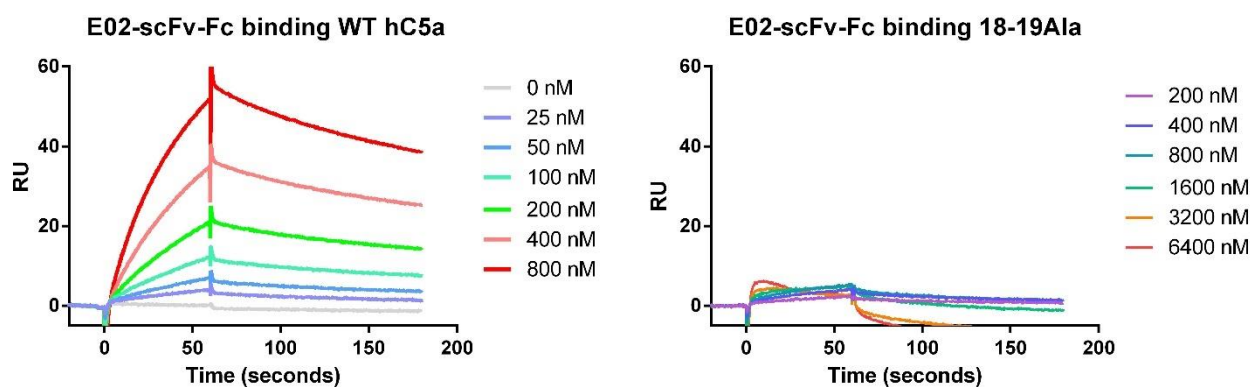


**Fig. S22. Binding affinities of E02-scFv-Fc fusion proteins on WT hC5a and alanine mutant, measured by Biacore T100.**

The  $k_a$ ,  $k_d$ , and  $K_D$  of E02-scFv-Fc on hC5a are  $3.1E04$  1/M.s,  $3.0E-03$  1/s,  $9.6E-08$  M, respectively. The on-rate, off-rate, and binding constant on 18-19Ala mutant could not be deduced due to weak binding affinity.

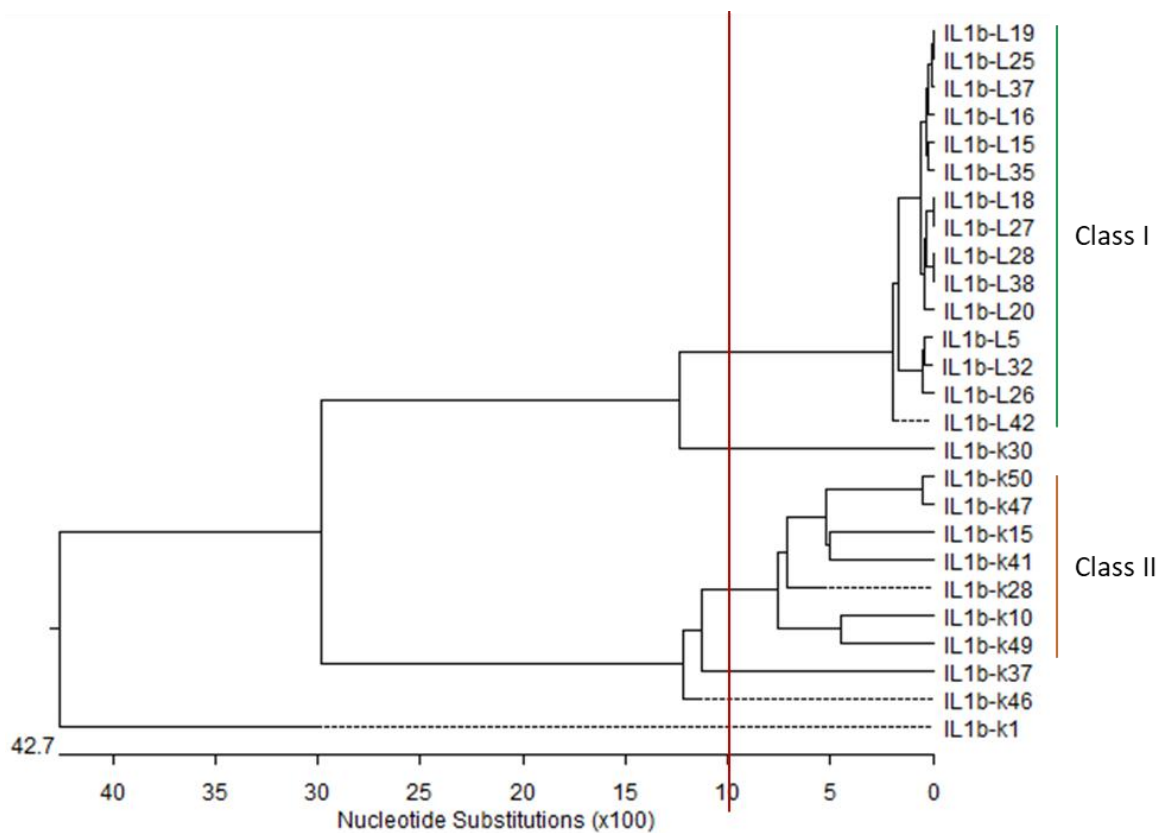


**Fig. S23. Sequence analysis of the hit pool from panning phage library generated from mouse immunization of IL1 $\beta$  against 64pBpa using a conventional method.**

Two sequence clusters were identified based on homology (with at least two homologous sequences when 10x100 nucleotide substitutions cutoff was applied).



**Table S1.** UV/non-UV output ratio of hit pools from panning a human naïve antibody phage library against 63pBpa and 64pBpa. The results listed in the table were from an independent repeat of the experiment shown in Table 1.

<b>Sample</b>	<b>UV output (cfu)</b>	<b>non-UV output (cfu)</b>	<b>UV/non-UV output ratio</b>
Hit pool from panning against 64pBpa	543	187	*2.9
Hit pool from panning against 63pBpa	1297	407	*3.2
Canakinumab-scFv phage against 63pBpa (Positive phage control)	13600	4100	*3.3
Gevokizumab-scFv phage against 63pBpa (Negative phage control)	25000	31000	0.8
Hit pool from panning against WT IL1 $\beta$ (Negative antigen control)	873	760	1.1

The *p* value of pBpa mutant group or positive phage control group vs negative antigen control group. \**p*<0.05. The statistical analysis was based on the UV/non-UV output ratios listed in Table 1 and Table S1.

**Table S2.** UV/non-UV output ratio of monoclonal phages from panning human naïve phage library against 63pBpa, 64pBpa or WT IL1 $\beta$ . 0.1  $\mu$ g/well proteins were coated. The results in A and B were from two independent experiment repeats under the same condition.

(A)

Sample	UV output (cfu)	non-UV output (cfu)	UV/non-UV output ratio
63UV7 phage against 63pBpa	201	46	*4.4
64UV63 phage against 64pBpa	140	22	*6.4
63UV7 phage against WT IL1 $\beta$ (Negative antigen control)	184	197	0.9
64UV63 phage against WT IL1 $\beta$ (Negative antigen control)	128	117	1.1
Gevokizumab-scFv phage against 63pBpa (Negative phage control)	4000	3040	1.3
Canakinumab-scFv phage against 63pBpa (Positive phage control)	7900	2120	*3.7

(B)

Sample	UV output (cfu)	non-UV output (cfu)	UV/non-UV output ratio
63UV7 phage against 63pBpa	133	32	*4.2
64UV63 phage against 64pBpa	124	26	*4.8
63UV7 phage against WT IL1 $\beta$ (Negative antigen control)	126	148	0.9
64UV63 phage against WT IL1 $\beta$ (Negative antigen control)	115	132	0.9
Gevokizumab-scFv phage against 63pBpa (Negative phage control)	8600	6100	1.4
Canakinumab-scFv phage against 63pBpa (Positive phage control)	6700	2400	*2.8

The *p* value of pBpa mutant group vs negative antigen control group and positive phage control group vs negative phage control group. \**p*<0.05. The statistical analysis was based on the UV/non-UV output ratios listed in Table S2A and S2B.

**Table S3.** UV/non-UV output ratio of the hit pool and monoclonal phages from panning an antibody phage library (generated by mouse immunization) against 64pBpa. The results listed in the table were from an independent repeat of the experiment shown in Table 2.

<b>Sample</b>	<b>UV output (cfu)</b>	<b>non-UV output (cfu)</b>	<b>UV/non-UV output ratio</b>
Hit pool from panning against 64pBpa	4300	842	*5.1
i64UV9 phage	2360	285	*8.2
i64UV120 phage	4600	1700	*2.7
i64UV5 phage	1360	1250	<sup>ns</sup> 1.1
i64UV40 phage	5700	7200	<sup>ns</sup> 0.8
i64UV104 phage	1760	1200	<sup>ns</sup> 1.5
i64UV110 phage	548	687	<sup>ns</sup> 0.8

The *p* value of pBpa mutant group vs negative antigen control group (in Table S4). \**p*<0.05, <sup>ns</sup>*p*≥0.05. The statistical analysis was based on the UV/non-UV output ratios listed in Table 2, Table S3, and Table S4.

**Table S4.** UV/non-UV output ratio of the hit pool and monoclonal phages from panning immunization library against WT IL1 $\beta$ . 0.1  $\mu$ g/well proteins were coated. The results in A and B were from two independent experiment repeats under the same condition, which represents the negative antigen control groups of Table 2 and Table S3.

(A)

<b>Sample</b>	<b>UV output (cfu)</b>	<b>non-UV output (cfu)</b>	<b>UV/non-UV output ratio</b>
Hit pool from panning against WT IL1 $\beta$	476	432	1.1
i64UV9 phage	1400	1500	0.9
i64UV120 phage	2500	2300	1.1
i64UV5 phage	453	402	1.1
i64UV40 phage	8300	8000	1.0
i64UV104 phage	1600	1200	1.3
i64UV110 phage	1440	1350	1.1

(B)

<b>Sample</b>	<b>UV output (cfu)</b>	<b>non-UV output (cfu)</b>	<b>UV/non-UV output ratio</b>
Hit pool from panning against WT IL1 $\beta$	641	684	0.9
i64UV9 phage	960	940	1.0
i64UV120 phage	2200	2100	1.0
i64UV5 phage	850	710	1.2
i64UV40 phage	4700	5400	0.9
i64UV104 phage	1300	920	1.4
i64UV110 phage	1350	1460	0.9

**Table S5.** UV/non-UV output ratio of hit pools from panning immunization library against 18pBpa and WT hC5a. 0.1 µg/well proteins were coated. The results in A and B were from two independent experiment repeats under the same condition.

(A)

Sample	UV output (cfu)	non-UV output (cfu)	UV/non-UV output ratio
Hit pool from panning against 18pBpa	370	28	*13.2
Hit pool from panning against WT hC5a (Negative antigen control)	42	34	1.2

(B)

Sample	UV output (cfu)	non-UV output (cfu)	UV/non-UV output ratio
Hit pool from panning against 18pBpa	862	55	*15.7
Hit pool from panning against WT hC5a (Negative antigen control)	435	297	1.5

The *p* value of pBpa mutant group vs negative antigen control group. \**p*<0.05. The statistical analysis was based on the UV/non-UV output ratios listed in Table S5A and S5B.